nature microbiology

ARTICLES

https://doi.org/10.1038/s41564-020-0781-2

Fluoxazolevir inhibits hepatitis C virus infection in humanized chimeric mice by blocking viral membrane fusion

Christopher D. Ma[1], Michio Imamura[2], Daniel C. Talley[3], Adam Rolt[1], Xin Xu[3], Amy Q. Wang[3], Derek Le[1], Takuro Uchida[2], Mitsutaka Osawa[2], Yuji Teraoka[2], Kelin Li[4], Xin Hu[3], Seung Bum Park[1], Nishanth Chalasani[1], Parker H. Irvin[1], Andres E. Dulcey[3], Noel Southall[3], Juan J. Marugan[3], Zongyi Hu[1], Kazuaki Chayama[2], Kevin J. Frankowski[4] and Tsanyang Jake Liang[1]✉

Fluoxazolevir is an aryloxazole-based entry inhibitor of hepatitis C virus (HCV). We show that fluoxazolevir inhibits fusion of HCV with hepatic cells by binding HCV envelope protein 1 to prevent fusion. Nine of ten fluoxazolevir resistance-associated substitutions are in envelope protein 1, and four are in a putative fusion peptide. Pharmacokinetic studies in mice, rats and dogs revealed that fluoxazolevir localizes to the liver. A 4-week intraperitoneal regimen of fluoxazolevir in humanized chimeric mice infected with HCV genotypes 1b, 2a or 3 resulted in a 2-log reduction in viraemia, without evidence of drug resistance. In comparison, daclatasvir, an approved HCV drug, suppressed more than 3 log of viraemia but is associated with the emergence of resistance-associated substitutions in mice. Combination therapy using fluoxazolevir and daclatasvir cleared HCV genotypes 1b and 3 in mice. Fluoxazolevir combined with glecaprevir and pibrentasvir was also effective in clearing multidrug-resistant HCV replication in mice. Fluoxazolevir may be promising as the next generation of combination drug cocktails for HCV treatment.

Hepatitis C virus (HCV) is a positive-sense, single-stranded, 9.6-kb virus in the Flaviviridae family that infects over 70 million people worldwide[1]. HCV is one of the leading causes of liver cirrhosis, hepatocellular carcinoma and liver failure[2]. Once exposed to the virus, patients may remain asymptomatic for months, thereby impeding the treatment-seeking process[3]. Since interferon was first tested in the 1980s, the cure rate of HCV has steadily improved with the development of direct-acting antivirals (DAAs)[4,5]. A combination of first-generation DAAs with PEGylated interferon-α and ribavirin was first approved in 2011, elevating the cure rate to nearly 90% from about 50% with just PEGylated interferon and ribavirin[4,5]. Current DAA combination regimens are more effective with fewer side effects and have a higher barrier to drug resistance, improving the sustained virological response (SVR) rate to more than 90%[4,5].

Despite this progress, there are still areas of unmet need in HCV therapy. Many individuals infected with HCV do not have access to existing treatments because of high costs[6]. Also, DAA therapy is less effective in difficult-to-treat patients, such as genotype 3 HCV infection with or without cirrhosis[7]. New and unusual subtypes (non-1a/1b, 3b, 4r) have also been discovered in patients from Asia and Africa and are less responsive to the current pan-genotypic regimen, sofosbuvir/velpatasvir, with a 50% SVR[8–10]. DAAs and other commonly used drugs have undesirable side effects and drug–drug interactions[11]. Many current treatment durations are lengthy at 12–24 weeks, although, in some cases, 8 weeks may suffice[12]. Shorter treatment durations may reduce costs and improve compliance. Finally, the emergence and transmission of HCV strains with multidrug resistance-associated substitutions (RASs) are a growing concern since they are less responsive to DAA retreatment[13–15,16]. In some studies, the response to retreatment is lower than 50% due to these multidrug RASs[14]. HCV reinfection occurs invariably in the transplant setting; effective preventive treatment, such as the use of hepatitis B immunoglobulin in preventing hepatitis B virus reinfection after liver transplant, would be valuable[17]. Therefore, new antivirals are needed to improve treatment efficacy and shorten treatment duration.

We previously identified a promising aryloxazole-based series of HCV entry inhibitors, which have a structural scaffold different from other described HCV entry inhibitors[18]. After further structure–activity relationship optimization, we identified the compound 18a (NCGC00351982 or fluoxazolevir) as the lead candidate for preclinical development based on the best combined profile of efficacy, cytotoxicity and in vitro absorption, distribution, metabolism and excretion (half maximal effective concentration (EC_{50}) = 0.0188 μM, 50% cytotoxic concentration (CC_{50}) = 13.0 μM, selectivity index $CC_{50}/EC_{50} > 600$)[19]. We report here the mechanism of action of fluoxazolevir, including in vitro efficacy against various HCV genotypes, synergy with U.S. Food and Drug Administration-approved HCV drugs, in vivo pharmacokinetics in mice, rats and dogs, and efficacy in a humanized chimeric mouse model against HCV genotype 1b, 2a or 3 infection.

Results

Fluoxazolevir inhibits HCV fusion with hepatic cells. In a previous study, fluoxazolevir (Fig. 1a) was shown to target the entry step

[1]Liver Diseases Branch, National Institute of Diabetes and Digestive and Kidney Diseases, National Institutes of Health, Bethesda, MD, USA. [2]Department of Gastroenterology and Metabolism, Graduate School of Biomedical & Health Science, Hiroshima University, Hiroshima, Japan. [3]Division of Preclinical Innovation, National Center for Advancing Translational Sciences, National Institutes of Health, Rockville, MD, USA. [4]Center for Integrative Chemical Biology and Drug Discovery, University of North Carolina Eshelman School of Pharmacy, Chapel Hill, NC, USA. ✉e-mail: jliang@nih.gov

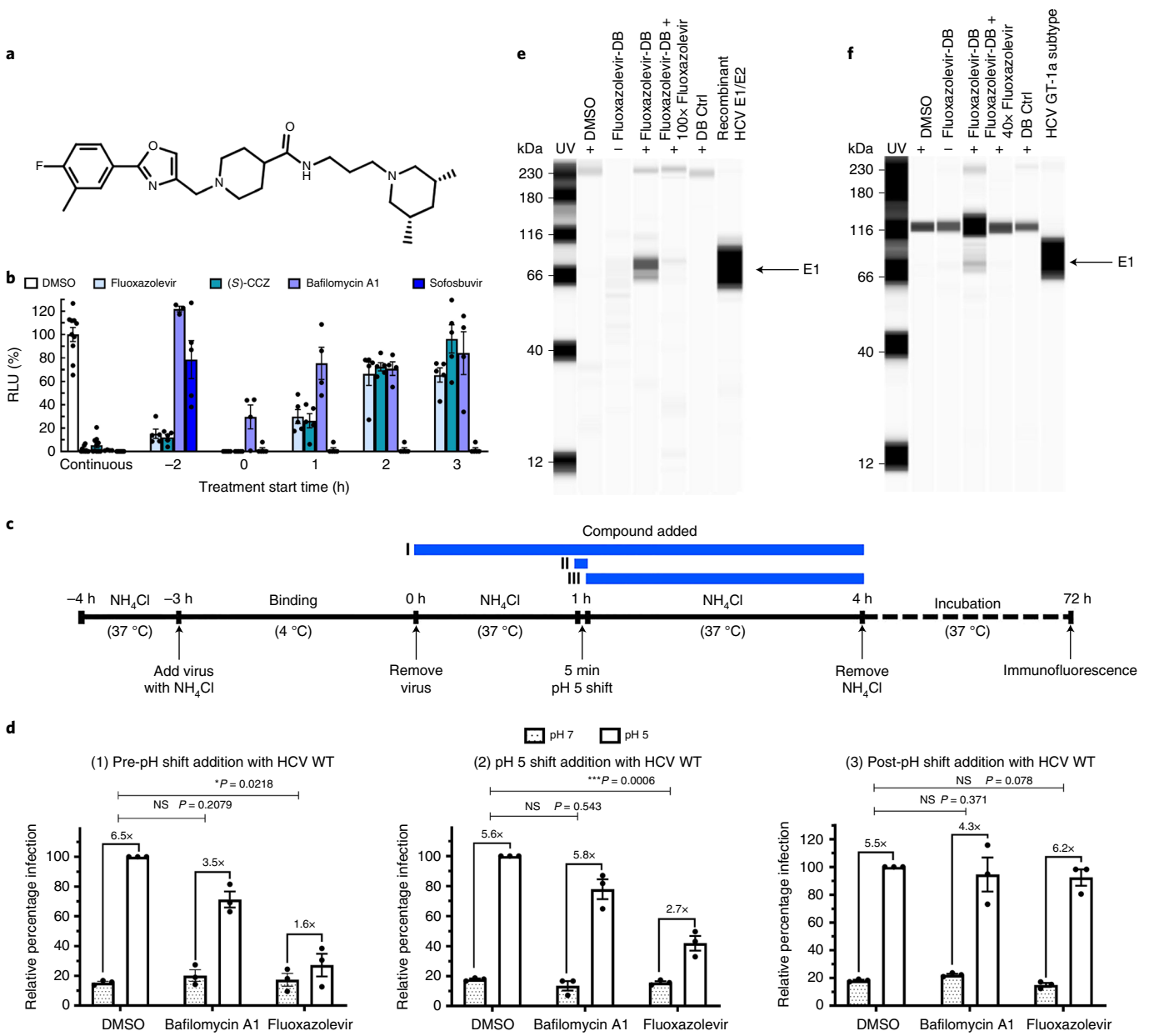

Fig. 1 | Fluoxazolevir disrupts HCV membrane fusion. a, The structure of fluoxazolevir. **b**, A time-of-addition assay was performed with fluoxazolevir and other controls (see Methods). Results were normalized to the DMSO continuous treatment. Data are presented as mean values ± s.e.m. ($n = 4$–10 biological independent samples). RLU, relative luminescence unit. **c**, The membrane fusion assay scheme shows three protocols where the compound (fluoxazolevir, bafilomycin A1 or DMSO) was added at various time points (see Methods). **d**, Huh7.5.1 cells were stained by HCV core immunofluorescence. The numbers of HCV-positive foci (≥5 stained cells in each group) were counted in each well. Data were normalized to the DMSO continuous treatment and are presented as mean values ± s.e.m. ($n = 3$ biological independent samples). The statistical significance of the fold changes between the pH 7 and pH 5 shift was compared to the DMSO control within each protocol (two-sided Student's *t*-test). NS, not significant. **e**, Fluoxazolevir-DB was used in a cross-linking experiment with genotype 1a recombinant HCV E1/E2 protein (see Methods in Supplementary Information). Recombinant E1/E2 protein was included on the blot as a reference. **f**, After the addition of fluoxazolevir-DB to HCV genotype 1a-infected Huh7.5.1 cells, cells were subjected to ultraviolet cross-linking and lysis (see Methods). The high-titre HCV genotype 1a virus generated in the cell culture was included on the blot as a reference. In one sample, an excess amount of fluoxazolevir (200 μM) was added with fluoxazolevir-DB (2 μM for in vitro and 5 μM for infected cells) before the cross-linking reaction. The results are representative of three independent experiments.

of the HCV life cycle using an HCV pseudoparticle assay[19]. To confirm fluoxazolevir's role in inhibiting HCV entry, a time-of-addition assay was performed[20]. Bafilomycin A1, a vacuolar-type H^+-ATPase inhibitor, (*S*)-CCZ, a previously identified HCV late entry inhibitor[20] and sofosbuvir, an NS5B polymerase inhibitor, were used as controls. Overall, fluoxazolevir showed a similar pattern of HCV inhibition to that of (*S*)-CCZ (Fig. 1b). Both fluoxazolevir and (*S*)-CCZ displayed potent inhibition similar to the continuous treatment when added either simultaneously or 2 h before infection. When fluoxazolevir and (*S*)-CCZ were administered 1 h after infection, both compounds were still effective in inhibiting infection. Bafilomycin A1 behaved similarly, but when added either 2 h before

or 1 h after infection, it was much less effective, suggesting a more transient effect. In contrast, sofosbuvir was completely ineffective when the treatment was administered 2 h before infection but very potent when added simultaneously or any time after infection. The time-of-addition assay confirmed that fluoxazolevir targets the entry stage of the HCV life cycle.

A membrane fusion assay was performed to define whether fluoxazolevir targets viral fusion or another viral entry step (Fig. 1c)[21]. To prevent premature endosomal acidification, and consequently HCV entry, 10 mM of NH_4Cl was added in all solutions throughout the assay[22]. Cell receptor binding was synchronized when high-titre HCV with NH_4Cl was added to cells for 3 h at 4 °C (ref. [23]). Forced HCV internalization and fusion with cytosolic lysosomes were then triggered by changing the overall pH of the medium to pH 5 for 5 min. After the pH shift, cells were incubated at 37 °C for 3 h, washed, cultured in regular media without NH_4Cl for 72 h and then analysed for infection rate.

In the fusion assay (Fig. 1c,d), compounds were added at various times to test for specificity in inhibiting viral fusion. In protocols I and II, bafilomycin A1 behaved similarly to the dimethyl sulfoxide (DMSO) control treatment. As expected, the artificial lowering of the cytosolic pH overcame the block of endosomal acidification by bafilomycin A1, thus allowing HCV fusion to occur[23]. In contrast, HCV infection only increased minimally by 1.6-fold after the pH shift in the fluoxazolevir treatment group, which was lower than the increases of the DMSO (6.5-fold) and bafilomycin A1 (3.5-fold) groups. This finding indicates that fluoxazolevir blocks viral fusion within the endosomes even under an acidic environment. In protocol III, both fluoxazolevir and bafilomycin A1 failed to inhibit HCV infection since the compounds were added after the viral fusion step. Altogether, fluoxazolevir specifically inhibits the fusion step of HCV entry.

Fluoxazolevir binds to the HCV envelope protein 1 (E1). To investigate the target of fluoxazolevir, a fluoxazolevir-diazirine-biotin (fluoxazolevir-DB) probe was synthesized (Extended Data Fig. 1a). Fluoxazolevir-DB showed inhibition against HCV infection in a dose-dependent manner with an EC_{50} of 1.19 μM (Extended Data Fig. 1b) and was stable at room temperature and under ambient light with slow decomposition after a few days (Extended Data Fig. 1c,d). When performing the fluoxazolevir-DB cross-linking experiment with recombinant HCV E1/E2 proteins under ultraviolet irradiation, the activated cross-linked product was identified to be the E1 protein by western blot with anti-E1 antibody (Fig. 1e). Under various control conditions, such as fluoxazolevir-DB without ultraviolet activation, DMSO and a sample with excess fluoxazolevir (200 μM) to compete against fluoxazolevir-DB (2 μM), the E1 protein was not detected. A similar ultraviolet cross-linking experiment was performed with fluoxazolevir-DB (5 μM) and Huh7.5.1 cells infected with high-titre chimeric genotype 1a HCV and showed specific cross-linking of fluoxazolevir-DB to E1 (Fig. 1f).

Fluoxazolevir RASs in E1. To further study the mechanism of action and genetic barrier to drug resistance of fluoxazolevir, an in vitro drug-induced resistance selection assay was performed[24]. Fluoxazolevir resistance emerged after 21 passages (Supplementary Fig. 1) compared to 11 passages for the NS5A inhibitor daclatasvir (Supplementary Fig. 2), indicating that fluoxazolevir may have a higher genetic barrier to resistance than daclatasvir. Amplified viruses from some of these passages (wells A1, B1, C1, E1, G1 and H1) showed a substantial shift of fluoxazolevir dose–response curves (an increase of EC_{50} > twofold), indicating the generation of the fluoxazolevir RASs (Extended Data Fig. 2). It is not clear why amplified viruses from other passages (wells D1 and F1) did not show any substantial resistance to fluoxazolevir. It is possible that certain RASs may have been less fit and promptly reverted to the wild-type (WT) sequence in the final amplification passage, when the compound was not added. Sequencing of the core, E1 and E2 regions of the viral isolates at the last stage of each selection passage identified various potential RASs (Fig. 2a,b), which were validated in the amplified viral stock. In the selection assay with daclatasvir (Supplementary Fig. 2), a common RAS (NS5A F28C) was found[15,25], supporting the validity of this assay.

Mutations were then introduced individually into the HCV WT genome to confirm their resistance against fluoxazolevir. The mutant viral clones replicated similarly (no more than 20% difference) to the HCV WT clone (Extended Data Fig. 3a,b). Analysis of infectious virus production in the culture supernatant showed that most RAS-containing viruses produced similar levels of infectious virus in comparison to the HCV WT except for two E2 mutants: M405V and P616A, which produced somewhat lower infectious viral titres, and V414A, which produced more infectious virus (Extended Data Fig. 3a,c). The E1 RASs showed minor to moderate resistance (Fig. 2c,d and Extended Data Fig. 4). Among them, A274S, I374T, D382E and V414A exhibited notable resistance with the EC_{50} shifting from 36.7 nM against the HCV WT to 201, 242, 169 and 176 nM, respectively. Many of the mutations clustered in the E1 fusion peptide sequence, supporting the concept that fluoxazolevir targets the HCV fusion process. Two E1 mutations (I374T and D382E) occurred outside the fusion peptide and showed resistance (Fig. 2c). Mutations in the E2 protein (T395A, M405V, P616A) were also detected but they all occurred in the presence of validated resistant E1 mutations; when tested individually, they did not show much resistance (Fig. 2c and Extended Data Fig. 4).

Fluoxazolevir inhibits HCV chimeric infection. Dose–response assays of fluoxazolevir were performed against all chimeric HCV-*Renilla* luciferase (RLuc) genotypes including 1a, 1b, 2b, 3a, 4a, 5a, 6a and 7a (Fig. 3)[26] and compared to the J6/JFH1 HCV-RLuc (genotype 2a). Fluoxazolevir was generally effective against all HCV genotypes and reached a maximum inhibition close to 100% at concentrations below notable toxicity. Fluoxazolevir showed genotypic variations in efficacy with varying EC_{50} values. It was most effective against HCV 2a and 2b, followed by 3a and 6a, all within sub-μM EC_{50} values. Fluoxazolevir also displayed little to no cytotoxicity, with CC_{50} > 20 μM in primary human hepatocytes, MT-4 cells, HepG2 cells and peripheral blood mononuclear cells (Extended Data Fig. 5), and approximately 12 μM in Huh7.5.1 cells (Fig. 3).

Fluoxazolevir synergizes with other anti-HCV drugs. To explore the potential combination of fluoxazolevir with currently available anti-HCV drugs, we tested the synergistic antiviral effects of fluoxazolevir with human interferon-α, ribavirin, daclatasvir, sofosbuvir and simeprevir (NS3/4A protease inhibitor). Two commonly used programs to calculate synergy, CalcuSyn and MacSynergy II, were applied[27]. CalcuSyn calculates combination indices (CIs) by analysing the inhibitory effects near the EC_{50} values for each drug[28], while MacSynergy II uses the Bliss independence model[29]. Both programs use different definitions to determine the level of synergy; thus, each program provides a different but complementary profile of synergistic analysis. Drug combinations were added in a dose-dependent manner to determine whether the inhibitory effects of the treatment were synergistic, additive, equal or antagonistic to the inhibitory effects of each drug independently. CalcuSyn showed that fluoxazolevir was highly synergistic with all five selected antivirals while MacSynergy II demonstrated varying extents of synergism (Table 1).

Pharmacokinetic and toxicity studies in animal models. After single-dose administration in mice and rats, fluoxazolevir showed preferential localization in the liver with long $t_{1/2}$ values for both intravenous and oral routes: 17–37 h in the plasma and 26–45 h in

a

Well Location (passage no.)	Region	Mutations
A1 (p27)	Core	V140L
	E1	F291L
	E2	V414A
B1 (p27)	Core	R9G
	E1	I374T
	E2	None
C1 (p27)	Core	None
	E1	D382E
	E2	T395A, M405V, P616A
D1 (p27)	Core	None
	E1	None
	E2	None
E1 (p27)	Core	None
	E1	F291V
	E2	None
F1 (p27)	Core	None
	E1	None
	E2	None
G1 (p27)	Core	None
	E1	A274S
	E2	None
H1 (p27)	Core	None
	E1	M267V, V284A
	E2	None

b

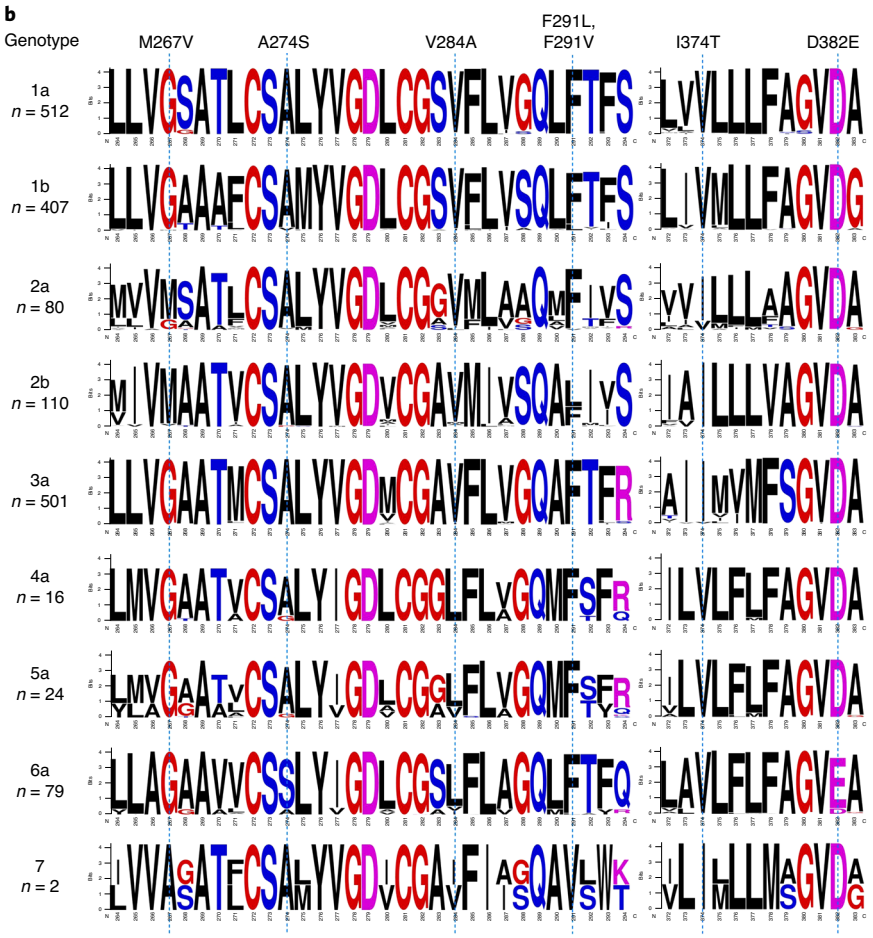

c

HCV	Fluoxazolevir		Sofosbuvir	
	EC_{50}(μM)	Maximal response ± s.e.m. (%) at 1 μM	EC_{50}(μM)	Maximal response ± s.e.m. (%) at 10 μM
WT	0.037	93.3 ± 1.1	0.053	100 ± 0
R9G	0.064	92.9 ± 1.0	0.040	100 ± 0
V140L	0.078	93.3 ± 1.1	0.044	100 ± 0
M267V	0.102	90.4 ± 1.5	0.056	100 ± 0
V284A	0.040	92.3 ± 0.8	0.055	100 ± 0
A274S	0.201	78.2 ± 5.2	0.045	100 ± 0
F291L	0.127	88.9 ± 1.8	0.054	100 ± 0
F291V	0.104	87.9 ± 1.8	0.045	100 ± 0
I374T	0.242	93.3 ± 1.1	0.080	100 ± 0
D382E	0.169	87.5 ± 0.8	0.062	100 ± 0
T395A	0.094	89.8 ± 1.4	0.035	100 ± 0
M405V	0.044	91.3 ± 1.6	0.049	100 ± 0
V414A	0.176	69.3 ± 3.3	0.046	100 ± 0
P616A	0.073	91.1 ± 1.7	0.052	100 ± 0

d

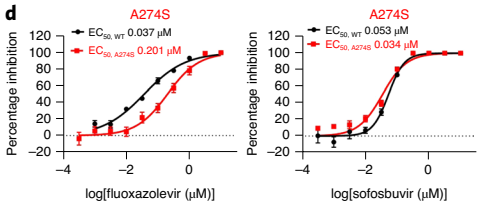

Fig. 2 | Fluoxazolevir-resistant HCV substitutions generated from the in vitro resistance selection assay. a, A fluoxazolevir concentration gradient was established in a 96-well plate with HCV J6/JFH1 where the concentrations were 5 μM in column 1 and 0 μM in column 12. Mutations that emerged in the vehicle-only control (Supplementary Fig. 1, column 12, DMSO) were not included because they most likely represented naturally evolved mutations with each passage. The detected mutations were I313V, N417S, I438V, L524F, I678V and L744S. **b**, Partial E1 sequences of all major genotypes, except for genotype 7, were obtained from the Virus Pathogen Resource database and were aligned between residues 264 and 294, and between residues 372 and 383. Genotype 7 sequences were obtained from the National Center for Biotechnology Information. The *n* of each genotype sequence in the analysis is shown. Putative E1 RASs against fluoxazolevir are indicated. MAFFT v.7 with the G-INS-1 progressive method and Berkeley WebLogo were used to generate the alignment figure. **c**, The EC_{50} values and maximal percentage inhibition responses are summarized for all the generated RASs against fluoxazolevir or sofosbuvir and further detailed in Extended Data Fig. 4. Fluoxazolevir inhibits HCV J6/JFH1 infection close to 100% at concentrations above 1 μM for all RASs, so the maximal response for each virus strain was reported at 1 μM. **d**, The representative dose–response curves of one RAS (A274S) against fluoxazolevir and sofosbuvir are shown here ($n = 6$ biologically independent samples) and the rest in Extended Data Fig. 4. Data are presented as mean values ± s.e.m.

the liver (Extended Data Figs. 6a,b and 7). When fluoxazolevir was administered intravenously (3 mg kg^{-1}), the volume of distribution at steady state (V_{dss}) was 137 l kg^{-1} and 12 ± 31 l kg^{-1} for CD-1 mice and Sprague Dawley rats, respectively. The high values of V_{dss} suggested that the compound penetrated tissues extensively. After oral administration (10 mg kg^{-1}), the C_{max} values in the plasma were 0.084 μM and 0.017 μM, the C_{max} values in the liver were 34.4 and 39.9 μM and the liver to plasma area under the curve (AUC) ratios were 659 and 6,250 for CD-1 mice and Sprague Dawley rats, respectively (Extended Data Fig. 7). The oral bioavailabilities were 37 and 1.2% for CD-1 mice and Sprague Dawley rats, respectively, after a 10 mg kg^{-1} oral administration (Table 2).

In dogs, fluoxazolevir exhibited a similar pharmacokinetic profile as in rodents (Table 2 and Extended Data Fig. 6c), with a long $t_{1/2}$ via intravenous (3 mg kg^{-1} dose; 29 h) and oral (10 mg kg^{-1} dose; 19 h) routes, high plasma clearance (67 ± 6 ml min kg^{-1}), large V_{dss} (144 ± 151 kg) and bioavailability of 14%. Analysis of urine samples collected for 10 d after the intravenous dosing showed a total renal excretion of 2.3 ± 0.4% of the administered dose.

A single dose of fluoxazolevir in these animals did not show any evidence of liver injury (alanine aminotransferase elevation) or other notable toxicity (Extended Data Fig. 6d). The maximum tolerable dose in CD-1 mice was determined by administering a single dose of 50, 100, 500 or 1,000 mg kg^{-1} fluoxazolevir by oral gavage with daily assessment of toxicity (body weight, observation, mortality and necropsy) for 3 d (Extended Data Fig. 8). No evidence of toxicity at any of those doses was observed.

Fluoxazolevir suppresses HCV infection in humanized chimeric mice. The antiviral effect of fluoxazolevir was tested in human

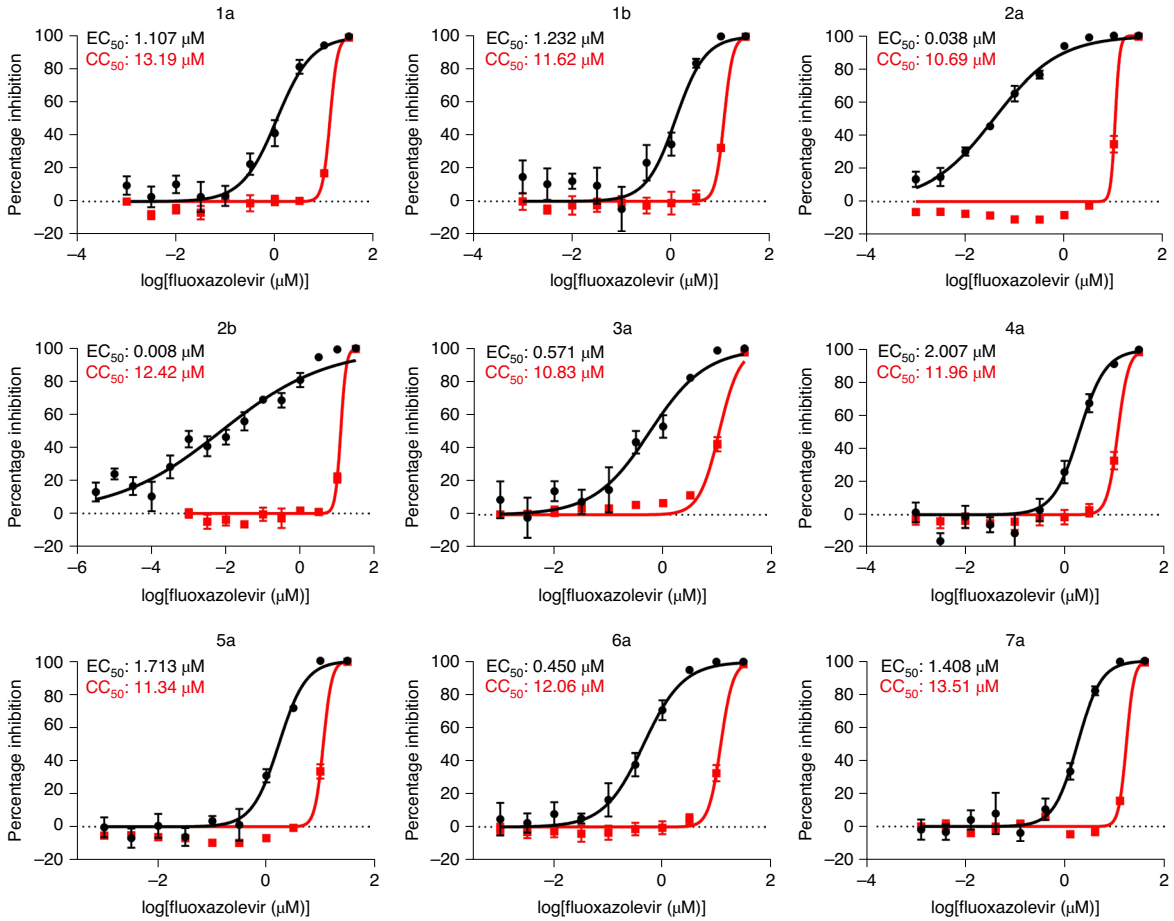

Fig. 3 | Dose–response curves of fluoxazolevir against various chimeric HCV genotypes. Huh7.5.1 cells in 96-well plates were infected with various chimeric HCV-RLuc genotypes (1a, 1b, 2a, 2b, 3a, 4a, 5a, 6a and 7a) together with fluoxazolevir at concentrations as indicated. Cells were collected 48 h after infection to assess luminescence via the luciferase assay (black circles). A parallel plate with the same treatment was processed for the ATPlite cytotoxicity assay (red squares). EC_{50} and CC_{50} values were calculated with Prism 7. Dose–response curves of J6/JFH1 HCV-RLuc (GT-2a) were used as a reference. Each data point was presented as the mean value ± s.e.m. of six biological independent replicates and the results are representative of three independent experiments.

Table 1 | Synergistic activity of fluoxazolevir with selected HCV drugs

Program	Parameter	Sofosbuvir	Ribavirin	Daclatasvir	Simeprevir	Interferon-α
CalcuSyn	CI value[a]	0.302 ± 0.019	0.375 ± 0.050	0.202 ± 0.078	0.421 ± 0.097	0.365 ± 0.051
	Synergy volume[b]	+++	+++	+++	+++	+++
MacSynergy II	log volume[c]	73.07	5.97	3.2	6.53	0.03
	Synergy volume[d]	+++	++	+	++	±

[a]CI values for CalcuSyn were determined by testing fluoxazolevir with the other therapies at or near their EC_{50} values when tested independently. [b]The synergy volume for CalcuSyn is defined as follows: +++ indicates strong synergy (CI < 0.7); ++ indicates moderate synergy (0.7 ≤ CI < 0.8); + indicates minor synergy (0.8 ≤ CI < 0.9); and ± indicates nearly additive (0.9 ≤ CI < 1.1). [c]The log volume for MacSynergy II is determined by the volumes of the peaks and valleys of the synergy/antagonism surface plots. [d]The synergy volume for MacSynergy II is defined as follows: +++ indicates strong synergy (log volume ≥ 9); ++ indicates moderate synergy (9 > log volume ≥ 5); + indicates minor synergy (5 > log volume ≥ 2); and ± indicates nearly additive (2 > log volume ≥ 0).

hepatocyte-engrafted *Alb-uPA/Scid* chimeric mouse models infected with HCV genotypes 1b, 2a or 3. Fluoxazolevir was administered intraperitoneally daily for 4 weeks in two dosing groups for genotypes 1b and 2a (0.1 mg kg^{-1} and 1 mg kg^{-1}) and one dosing group for genotype 3 (5 mg kg^{-1}), and the animals were followed off-treatment for an additional 4 weeks. During treatment, viral RNA levels steadily declined for all genotype infections treated with fluoxazolevir (Fig. 4a and Supplementary Fig. 3) compared to the untreated mice. The 1 mg kg^{-1} dose was more effective in genotype 1b-infected mice, which decreased the viral RNA titre by about 2 log, than in genotype 2a-infected mice, which decreased the viral titre by about 1 log. The 5 mg kg^{-1} dosage for genotype 3-infected mice had a decrease in viral RNA titre of approximately 1.5 log (Fig. 4b and Supplementary Figs. 4 and 5). Throughout the course of treatment, there was no evidence of viral rebound, but RNA levels rebounded after treatment ended. No RASs were identified after sequencing the virus before and after treatment, suggesting a high barrier of drug resistance in vivo (Supplementary Table 1). Finally, there was no evidence of toxicity during the course of treatment (Extended Data Fig. 9).

Table 2 | Pharmacokinetics of fluoxazolevir after 3 mg kg^{-1} intravenous and 10 mg kg^{-1} oral administration

Animal	CD-1 mouse[a,b] ($n=3$)		Sprague Dawley rat[a,b] ($n=3$)		Beagle dog[a] ($n=3$)	
Route (dose)	Intravenous (3 mg kg^{-1})	Oral (10 mg kg^{-1})	Intravenous (3 mg kg^{-1})	Oral (10 mg kg^{-1})	Intravenous (3 mg kg^{-1})	Oral (10 mg kg^{-1})
$AUC_{0-\infty}$ (μM h)	0.871	1.15	6.47 ± 4.17	0.268 ± 0.041	1.59 ± 0.13	0.753 ± 0.179
$t_{1/2}$ (h)	24	37	17	19	29	19
T_{max} (h)	-	2	-	0.3	-	0.8
C_{max} (μM)	-	0.084	-	0.042 ± 0.022	-	0.052 ± 0.017
CLp (ml min kg^{-1})	122	-	21 ± 10	-	67 ± 6	-
V_{dss} (l kg^{-1})	137	-	12 ± 3	-	144 ± 15	-
F (%)	-	37	-	1.2	-	14

[a]The plasma concentration of fluoxazolevir was measured after a single dose of fluoxazolevir via oral or intravenous route. [b]The s.d. could not be calculated since serial sampling was not performed with the mice. Three plasma samples were collected at each time point and a total of 39 mice and 15 rats in each treatment group were used for collection of tissue samples for the determination of the tissue pharmacokinetic profiles shown in Extended Data Fig. 7. $AUC_{0-\infty}$, AUC from zero to infinity; $t_{1/2}$, half-life; T_{max}, time to reach maximal concentration; C_{max}, maximal concentration after oral administration; CLp, plasma clearance; F, oral bioavailability.

Fluoxazolevir and daclatasvir combination therapy. Based on the synergy results and the demonstrated antiviral effects of fluoxazolevir in vivo, a 4-week combination therapy of fluoxazolevir and daclatasvir was conducted in humanized *Alb-uPA/Scid* mice infected with HCV genotype 1b or 3 to evaluate whether an SVR could be achieved. Monotherapy with daclatasvir was performed in comparison. The doses administered for fluoxazolevir and daclatasvir were 5 mg kg^{-1} intraperitoneally daily and 10 mg kg^{-1} orally daily, respectively. In the combination treatment of mice infected with both genotypes, the viral RNA levels in the serum rapidly decreased to undetectable levels without any evidence of emerging drug resistance and remained undetectable 4 weeks after stopping treatment, which is consistent with an SVR (Fig. 4b). On the other hand, daclatasvir monotherapy caused a rapid decline in viral levels, but the viraemia either never reached undetectable levels or rebounded, probably a result of emerging RASs. This study demonstrates that fluoxazolevir in combination with a DAA can achieve SVR against different HCV genotypes.

Human serum albumin levels were measured to monitor the engrafted human hepatocytes in all mice. During the entire course of treatment and follow-up, the human serum albumin levels remained relatively constant (Fig. 4a–d, Supplementary Figs. 3–5 and Extended Data Fig. 10), indicating that the reduction of HCV RNA was not caused by a loss of engrafted hepatocytes. One mouse from each treatment group infected by HCV genotype 1b showed a gradual decline of human serum albumin with time (Supplementary Fig. 4).

Fluoxazolevir is active against multidrug-resistant HCV. Mavyret, a combination of glecaprevir (a NS3/4A inhibitor) and pibrentasvir (an NS5A inhibitor), is a second-generation DAA regimen that is active against all HCV genotypes in vitro and in vivo and shows little or no loss of efficacy in commonly reported RASs[30–32]. Despite its high clinical efficacy, drug-resistant variants have been reported[33]. An HCV genotype 1b strain resistant to glecaprevir/pibrentasvir was generated in humanized chimeric mice infected with HCV genotype 1b by serial treatment with glecaprevir/pibrentasvir[34]. The virus contains NS3-D168E, a well-known NS3/4A RAS[31], and multiple NS5A RASs (Q24R, R30E, P58S and A92K). Humanized chimeric mice infected with this virus respond poorly to glecaprevir/pibrentasvir treatment; interestingly, the RASs persist in the mice despite the absence of treatment[34]. NS5A-P58S has been reported in Mavyret-treated HCV patients with disease relapse[33]. NS5A-R30E has not been reported but other RASs affecting this residue are known[32,35].

A 6-week combination therapy with fluoxazolevir and glecaprevir/pibrentasvir was conducted in humanized chimeric mice infected with this multidrug-resistant HCV strain. Fluoxazolevir was administered at a daily dose of 5 mg kg^{-1} while glecaprevir and pibrentasvir were administered at a daily dose of 60 mg kg^{-1} and 24 mg kg^{-1}, respectively. In addition, fluoxazolevir or glecaprevir/pibrentasvir was administered separately as monotherapy groups. Another group of infected mice was untreated and monitored for viraemia, which showed steady levels during follow-up (Extended Data Fig. 10a). Fluoxazolevir-treated mice showed a 1–2 log gradual decline of HCV viraemia (Fig. 4c, upper panel), similar to what was observed in mice infected with HCV WT genotypes 1b, 2a or 3. In glecaprevir/pibrentasvir-treated mice, HCV viraemia declined by 2–5 log but never reached an undetectable level, except for 1 time point in mouse HSB0190-0037 (Fig. 4c, middle panel). All mice rebounded to pretreatment viraemia levels after fluoxazolevir or glecaprevir/pibrentasvir was stopped. In combination-treated mice, HCV RNA decreased rapidly to undetectable levels and remained below detectable levels throughout the duration of treatment, indicating the effectiveness of fluoxazolevir together with glecaprevir/pibrentasvir in suppressing this multidrug-resistant variant (Fig. 4c, lower panel and Extended Data Fig. 10b). After stopping treatment, all three surviving mice continued to show undetectable levels of HCV RNA for a week. With a longer follow-up of 4 weeks, one mouse died, one showed a viral rebound and the third continued to have an undetectable level of HCV RNA. Sequence analysis of the virus in the mouse with post-treatment relapse showed the same drug-resistant substitutions in NS3 and 5A as the inoculum virus (Supplementary Table 1).

Acute HCV infection is delayed by fluoxazolevir. Since fluoxazolevir targets viral entry, it may potentially serve as an HCV preventive treatment. To determine the effectiveness of fluoxazolevir as a preventive therapy for HCV infection, a 1 mg kg^{-1} daily treatment was administered intraperitoneally for 5 d before and 2 weeks after HCV genotype 1b inoculation (Fig. 4d and Supplementary Fig. 6). In the control group without treatment, viral RNA levels increased to about 6 log a week after infection while the viral RNA levels for the pretreated group gradually increased only to about 3 log. After stopping treatment, HCV RNA levels steadily increased for both groups; however, the viral RNA levels of the preventive group were still significantly lower than those of the control group. These data suggest that an entry inhibitor, such as fluoxazolevir, can partially prevent and hinder the progression of de novo HCV infection in vivo.

Discussion

In generating fluoxazolevir-resistant HCV clones, we identified multiple mutations in the putative E1 fusion loop, a sequence spanning between amino acids 264 and 290 (refs. [36,37]), which

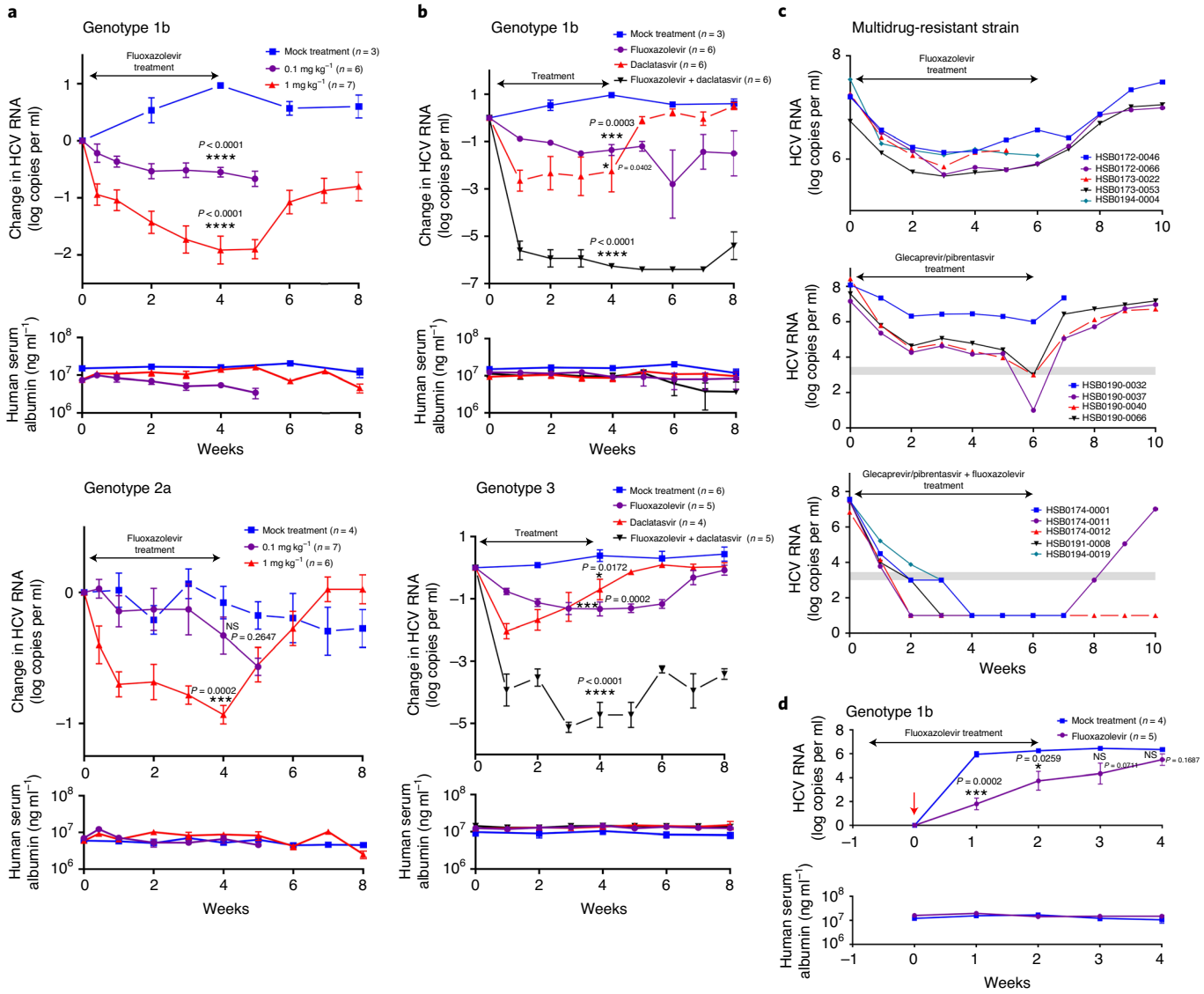

Fig. 4 | Efficacy of fluoxazolevir in vivo against HCV genotypes 1b, 2a and 3 and multidrug-resistant HCV infection in *Alb-uPA/Scid* mice. a, *Alb-uPA/Scid* mice infected with HCV genotype 1b or 2a were mock-treated or treated with 0.1 or 1 mg kg^{-1} of fluoxazolevir. **b**, Mice infected with genotype 1b or 3 were untreated or treated with 5 mg kg^{-1} of fluoxazolevir, 10 mg kg^{-1} of daclatasvir or both daily for 4 weeks. For the combination-treated mice, all samples from week 1 had serum HCV RNA levels below the quantification limit of 3.45 $\log_{10}$ copies per ml. Changes in HCV RNA levels from baseline were determined for each treated mouse and each data point is shown as the mean value ± s.e.m. The statistical significance of change in HCV viraemia at the end of treatment was compared to the mock-treatment control within each protocol (two-sided Student's *t*-test). Individual mouse data for **a** and **b** are shown in Supplementary Figs. 3–5. **c**, Mice were infected with a multidrug-resistant HCV strain and treated with 5 mg kg^{-1} fluoxazolevir, glecaprevir (60 mg kg^{-1})/pibrentasvir (24 mg kg^{-1}) or both daily for 6 weeks. The HCV viraemia of untreated infected mice and individual mouse serum albumin data are shown in Extended Data Fig. 10. Serum HCV RNA levels from individual mice are shown; graphs that end before 10 weeks are due to death of the mice. The grey area represents the lower limit of quantification (3.45 $\log_{10}$ copies per ml) and lower limit of detection (3 $\log_{10}$ copies per ml) for HCV RNA levels. **d**, A group of *Alb-uPA/Scid* mice were mock-treated or treated daily with 1 mg kg^{-1} of fluoxazolevir 5 d before and 2 weeks after HCV infection. The red arrow indicates time of infection. HCV RNA levels and human serum albumin were monitored weekly. The statistical significance of change in HCV viraemia at each time point is shown (two-sided Student's *t*-test). Individual mouse data are shown in Supplementary Fig. 6. The number of mice (*n*) for each experimental group of **a**,**b**,**d** is shown on the graph. Data are presented as mean values ± s.e.m.

confer drug resistance to fluoxazolevir. Two of the mutations were also induced by (*S*)-CCZ, another HCV fusion inhibitor (M267V and F291L)[38], but the other RASs were unique to fluoxazolevir (A274S and F291V). Therefore, selection of fluoxazolevir-resistant substitutions in the fusion peptide of E1 shows that fluoxazolevir blocks HCV entry by interrupting the viral fusion process. Fluoxazolevir-DB also binds directly to E1 through ultraviolet-activated cross-linking, further supporting that it interacts with E1 to prevent viral entry. Two E1 RASs (I374T and D382E) outside the fusion peptide in the distal transmembrane domain, potentially play a role in anchoring the transmembrane domain to the plasma membrane and the fusion process[39,40]. Both mutants also showed lower viral fitness in comparison to the WT, probably due to a disruption of structural integrity in this hydrophobic domain[41].

E2 interacts closely with E1 as a heterodimer[40] and may play a role in the fusion process[42] in addition to its interaction with host

entry factors. Thus, E2 mutations may contribute to resistance against fluoxazolevir. F345V/V414A mutations in HCV genotype 3a (S52 strain) were reported to enhance the release of infectious virus particles and confer resistance against interferon-α[43]. Increased viral fitness could account for the apparent drug resistance against the V414A mutant. Analyses of the replicating and infectious capacities of the described mutants show that many of them are less infectious than the WT, suggesting that these RASs are less fit and may not persist once the drug is removed.

Fluoxazolevir can achieve complete inhibition against all seven HCV chimeric genotypes in vitro with varying efficacies. Fluoxazolevir is most active against HCV genotypes 2a and 2b, which is not unexpected since HCV genotype 2a was used to discover fluoxazolevir[19]. The in vivo studies where fluoxazolevir is effective against genotypes 1b, 2a and 3 without the emergence of RASs support the broad genotypic coverage of fluoxazolevir. The pharmacokinetic studies demonstrated a favourable profile with high liver concentrations, long $t_{1/2}$ and reasonable oral bioavailability. With the dose administered, it was possible to achieve drug concentrations (>10 μM) in the liver that are substantially higher than the EC_{50} against all HCV genotypes without substantial toxicity.

Efficacy studies in humanized *Alb-uPA*/*Scid* mice showed that fluoxazolevir significantly suppressed HCV RNA levels during either monotherapy or combination therapy with daclatasvir. In mice infected with HCV genotypes 1b, 2a and 3, fluoxazolevir monotherapy decreased viral RNA significantly with no evidence of viral RNA rebound or generation of RASs. Daclatasvir monotherapy showed a greater decline in viral levels initially, which rebounded later during treatment, suggesting the emergence of RASs. In genotype 1b- or 3-infected mice treated with a combination of fluoxazolevir and daclatasvir, viral RNA levels were mostly below the detectable limit throughout the entire treatment period and 4 weeks after stopping treatment. Some of the post-treatment mice showed a detectable but not quantifiable HCV viraemia at some points after stopping treatment, which may represent residual non-infectious viral genomes after clearance since it does not lead to a substantial viral rebound.

A potent entry inhibitor, especially in combination with other DAAs, can minimize resistance and shorten treatment duration. Recent development of an entry inhibitor, myrcludex B, against chronic hepatitis D[44], is a case in point for this therapeutic strategy. Entry inhibitors may also potentially prevent or delay HCV graft reinfection in liver transplantation. Recent use of HCV-positive organs in HCV-negative recipients has presented a unique opportunity for pre-emptive therapy with DAAs to prevent infection[45,46]. Potentially, fluoxazolevir could be used at a higher dose or in combination with another DAA for this purpose.

In summary, we have shown that fluoxazolevir inhibits HCV entry by blocking membrane fusion of viral endosomes, which is also the mechanism of action for other recently described entry inhibitors, such as chlorcyclizine, flunarizine and 4-aminoquinoline derivatives[47–49]. Our preclinical studies support fluoxazolevir as a promising candidate for the next generation of drug cocktails for HCV treatment. It is synergistic with U.S. Food and Drug Administration-approved HCV antivirals, active against all HCV genotypes in vitro, has preferential localization in the liver, can clear various HCV strains in a humanized mouse model and has potential to delay or prevent acute HCV infection. Since the viral fusion structure and process is relatively conserved[50], it is also tempting to speculate that fluoxazolevir may have broader antiviral activities against other viruses.

Methods

Cells, chemicals and viruses. The HCV-permissive cell line Huh7.5.1 was maintained in DMEM (Thermo Fischer Scientific) with 10% FBS and antibiotics in a 37 °C and 5% CO_2 incubator. Cell lines were supplied from various sources: Huh7.5.1 cells, HepG2 cells, primary human hepatocytes (Thermo Fisher Scientific); MT-4 cells and peripheral blood mononuclear cells (National Institutes of Health (NIH), Department of Transfusion Medicine). All cell lines were regularly checked for *Mycoplasma* using the MycoAlert Mycoplasma Detection Kit (Lonza) and confirmed to be *Mycoplasma*-free. None of the cells were authenticated but they have been used extensively in our laboratory and behaved as expected. Fluoxazolevir was synthesized at the Center for Integrative Chemical Biology and Drug Discovery, University of North Carolina Eshelman School of Pharmacy and fluoxazolevir-DB was synthesized at the Chemical Genomics Center, National Center for Advancing Translational Sciences. (*S*)-CCZ was purified from racemic chlorcyclizine (Sigma-Aldrich)[20]. HCV inhibitors were purchased from various commercial sources: bafilomycin A1 (Sigma-Aldrich); sofosbuvir (Advanced ChemBlocks); ribavirin (Sigma-Aldrich); daclatasvir (Selleck Chemicals); simeprevir (Selleck Chemicals); and human interferon-α A (PBL Assay Science). HCV WT, HCV-RLuc (genotype 2a, J6-JFH1 clone) and various chimeric HCV-RLuc were generated according to the literature[26]. All constructs were confirmed via Sanger sequencing. HCV plasmids were linearized with XbaI (New England Biolabs), transcribed with the MEGAscript T7 Transcription Kit (Thermo Fischer Scientific) and electroporated into Huh7.5.1 cells with the Neon Transfection System at conditions of 1,400 V, 20 ms and 1 pulse (Thermo Fischer Scientific). The software program Omega v.1.10 (firmware v.1.21) was used to measure the luminescence readings of all RLuc assays.

Time-of-addition assay. Huh7.5.1 cells were seeded in 96-well plates (10^4 cells per well) and cultured overnight. HCV-RLuc (genotype 2a) were used to infect cells with the treatment of fluoxazolevir (10 μM) at various treatment times (continuous, −2, 0, 1, 2 and 3 h) as indicated in Fig. 1b. All treatments, except for the continuous group, were removed after 2 h of incubation and replaced with regular medium. Cells were further cultured for 48 h and then luminescence was assessed via the *Renilla* Luciferase Assay System (Promega Corporation). DMSO (Sigma-Aldrich), (*S*)-CCZ (10 μM), bafilomycin A1 (10 nM) and sofosbuvir (10 μM) were used in parallel to fluoxazolevir as controls.

Membrane fusion assay. The assay was modified from a method published previously (Fig. 1c)[48]. Huh7.5.1 cells were seeded in 96-well plates coated with 0.01% polylysine (Sigma-Aldrich; 1.5×10^4 cells per well) and cultured overnight at 37 °C. Cells were treated with NH_4Cl (10 mM) for 1 h at 37 °C before infection of WT J6-JFH1 HCV (0.5 multiplicity of infection) in the presence of NH_4Cl. Cells were incubated with the virus for 3 h at 4 °C and washed gently with medium containing NH_4Cl. Cells were incubated for 5 min at 37 °C with freshly prepared pH 5 or 7 citrate-phosphate buffer. Cells were incubated in medium containing NH_4Cl together with DMSO, 3 μM of fluoxazolevir or 3 nM of bafilomycin A1 in three protocols. In protocol I, the compound was added before the pH 5 shift and remained in solution until 3 h after the shift. In protocol II, the compound was added only during the pH shift. In protocol III, the compound was added after the pH shift and remained in the medium for 3 h. Cells were washed three times and cultured in regular DMEM for 72 h before being processed for HCV core immunofluorescence staining. HCV core-positive foci per well were recorded for the analysis of HCV infection under various conditions.

HCV core immunofluorescence staining. Huh7.5.1 cells were fixed with 4% paraformaldehyde diluted in phosphate-buffered saline (PBS) for 15 min and then blocked with 3% w/v bovine serum albumin (BSA) diluted in PBS with 0.3% v/v polysorbate 20. The anti-HCV core monoclonal antibody, which was generated from a 6G7 hybridoma clone and provided by H. Greenberg, was diluted in PBS by 1:500 v/v and used as the primary antibody. Alexa Fluor 488 anti-mouse antibody (Thermo Fischer Scientific) was diluted in PBS by 1:1,000 v/v and used as the secondary antibody. Cell nuclei were then stained with Hoechst dye (Thermo Fischer Scientific). Quantification of HCV infection was measured via fluorescence microscopy.

Ultraviolet-activated cross-linking and analysis of fluoxazolevir-DB and HCV E1 protein. In vivo ultraviolet-activated cross-linking was performed by infecting Huh7.5.1 cells (3×10^6) with high-titre HCV genotype 1a in a 10-cm dish and subsequently adding fluoxazolevir-DB (5 μM) or a control compound. Cells were incubated for 1 h at 37 °C and the mixture was exposed to ultraviolet irradiation for photoaffinity cross-linking. The medium was removed, cells were washed twice with 5 ml of cold PBS and 1 ml of lysis buffer (30 mM of Tris pH 7.5, 1 mM of EDTA, 150 mM of NaCl, 0.3% NP-40, 0.05% SDS); a protease inhibitor cocktail was then added. The cell lysate was pelleted via centrifugation at 20,000 relative centrifugal force (r.c.f.) at 4 °C for 5 min. The supernatant was isolated and kept at 4 °C before purification via Pierce NeutrAvidin agarose beads (Thermo Fisher Scientific).

The Pierce NeutrAvidin agarose beads were prepped before purification by spinning 50 μl of the beads down, discarding the supernatant and washing the beads with 1 ml of PBS twice. Biotin BSA (2 μl of 2 μg ml^{-1} biotin BSA in PBS) was added to the NeutrAvidin beads as a positive control. The cell lysate samples were then added to the beads, briefly mixed, placed on a rocker at 4 °C for 1 h and pelleted at 5,000 r.c.f. The beads were then washed twice with PBS followed by lysis buffer. After a final wash with PBS, elution buffer (2% SDS, 3 mM of biotin, 6 M of urea,

2 M of thiourea)[51], 1:4 Laemmli buffer and reducing agent were added to the beads, which were incubated for 10 min at room temperature and then again for 10 min at 95 °C. Samples were then centrifuged and the supernatant was used for western blot analysis via a Wes capillary western blot system (ProteinSimple). A4 anti-E1 antibodies (provided by H. Greenberg) were used for the western blot analysis.

In vitro drug-induced resistance selection assay. Huh7.5.1 cells were seeded in a black, clear bottom 96-well plate (10^4 cells per well), cultured overnight and then infected with WT J6/JFH1 HCV (1×10^5 focus forming units per ml) for 6 h to establish infection. After incubation, the viral medium was replaced with 200 µl of DMEM containing various fluoxazolevir concentrations per column on the plate, increasing by twofold from 10 nM to 5 µM (for example, 5 µM in column 1, 2.5 µM in column 2, and so on). Columns 11 and 12 contained DMSO treatment (0.1% v/v) as a vehicle-only control. After 72 h, a two-part infection was performed: (1) reinfection under the same fluoxazolevir concentration; and (2) challenge infection with a higher fluoxazolevir concentration (Supplementary Fig. 1). For the part-1 infection, 100 µl of virus-containing medium was transferred from well to well into another black, clear bottom 96-well plate seeded with uninfected Huh7.5.1 cells (10^4 cells per well). Each well in this plate contained the same concentration as the corresponding well in the original infected plate. For the part-2 infection, 50 µl of virus-containing medium was transferred to another black, clear bottom 96-well plate seeded with uninfected Huh7.5.1 cells with a final twofold higher fluoxazolevir concentration over the original well (for example, a well containing 2.5 µM of fluoxazolevir was passaged to a well containing 5 µM of fluoxazolevir). The remaining 50 µl of the original virus-containing medium was stored at −80 °C for further analyses. The part 1 infected cells were analysed via HCV core immunofluorescence staining to quantify productive infection for the previous passage. The two-part infection protocol was repeated every 3 d until positively infected cells were observed at 5 µM of fluoxazolevir. At this stage, the selected viral isolates were then amplified in the presence of fluoxazolevir to generate a stock for further analyses. The core, E1 and E2 regions of the viral isolates and their amplified viral stocks were sequenced (Fig. 2a). For the selection of daclatasvir-resistant variants, a concentration range of 10 pM to 5 nM was used.

In vivo pharmacokinetics. Male CD-1 mice and Sprague Dawley rats were obtained and maintained at the NIH animal facilities where all protocols were followed by the Division of Veterinary Resources and the Animal Care and Use Committee at the NIH. The pharmacokinetic studies in male beagle dogs were conducted by the Charles River Laboratories under their Institutional Animal Care and Use Committee approved protocol (no. PS-0002-DA-DE). All mice, rats and dogs used in the pharmacokinetics studies were selected randomly and no animals were given preferential treatment when allocating them into the experimental groups. Sample size was chosen based on the minimum number needed for statistical analysis.

The dosing solution of fluoxazolevir was freshly prepared before drug administration in 10% polyethylene glycol, 10% ethanol and 16% 2-hydroxypropyl-β-cyclodextrin for the intravenous and oral routes. The pharmacokinetic data were evaluated after a single dose at the stated route (that is oral gavage, intravenous injection). Blood, liver, brain and heart samples from the CD-1 mice, blood and liver samples from the Sprague Dawley rats, and blood and urine samples from the dogs were collected at various time points post-administration. Three samples ($n = 3$) were collected at each time point. Collected samples were immediately frozen and stored at −80 °C before analysis. Fluoxazolevir concentrations in the plasma, liver, brain, heart and urine were measured using ultraperformance liquid chromatography–tandem mass spectrometry. The pharmacokinetic parameters were presented as the mean ± s.d. for rats ($n = 3$, plasma) and dogs ($n = 3$). Pharmacokinetic parameters were derived using a non-compartmental method with Phoenix WinNonLin v.6.2.0 (Certara)[47].

In vivo efficacy studies in a humanized chimeric mouse model. A humanized chimeric mouse model was used to test the efficacy of fluoxazolevir in vivo against HCV in three experimental formats: monotherapy; combination therapy with daclatasvir or Mavyret (glecaprevir/pibrentasvir); and preventive therapy. HCV infection was established by infecting human HCV serum samples containing either genotype 1b, 2a or 3, or mouse serum samples containing the multidrug-resistant HCV strain (10^5 HCV copies) in *Alb-uPA*/*Scid* mice engrafted with primary human hepatocytes provided by PhoenixBio. Serum HCV RNA was monitored in mice for 6 weeks before treatment. Serum HCV titres were monitored weekly in HCV-infected chimeric mice before and after treatment with various regimens of fluoxazolevir (intraperitoneal). Human albumin levels in mouse serum were measured in parallel to monitor the grafted human hepatocytes[47]. The experiments were conducted at Hiroshima University under approved animal protocols. All mice in the in vivo efficacy studies were selected randomly and were not given preferential treatment when allocating them to the control or experimental groups. The sample size for each group was chosen based on availability of the animals at the time of the study.

Statistical analysis. Data were analysed with Prism 7 (GraphPad Software) and presented as the means ± s.e.m. ($n \geq 3$). Two-sided *t*-tests were used to determine the statistical difference between the means of two groups when sample sizes were small. Two-sided *P* values were also used in all analyses and $P < 0.05$ was considered statistically significant.

Reporting Summary. Further information on research design is available in the Nature Research Reporting Summary linked to this article.

Data availability

The data used to generate the HCV E1 alignment in Fig. 2b and support the findings of this study are available from the Virus Pathogen Resource database (genotypes 1–6). The two genotype 7 sequences are available in the National Center for Biotechnology Information with accession nos. YP_009272536 and ARB18146. The source data for Figs. 1b,d–f, 3 and 4, and Extended Data Figs. 1b, 2, 3b,c and 4–10 are included in the article. Other data supporting the findings of this study are available from the corresponding author upon request.

Received: 9 May 2020; Accepted: 27 July 2020;
Published online: 31 August 2020

References

1. Blach, S. et al. Global prevalence and genotype distribution of hepatitis C virus infection in 2015: a modelling study. *Lancet Gastroenterol. Hepatol.* **2**, 161–176 (2017).
2. Jafari, S., Copes, R., Baharlou, S., Etminan, M. & Buxton, J. Tattooing and the risk of transmission of hepatitis C: a systematic review and meta-analysis. *Int. J. Infect. Dis.* **14**, e928–e940 (2010).
3. Blackard, J. T., Shata, M. T., Shire, N. J. & Sherman, K. E. Acute hepatitis C virus infection: a chronic problem. *Hepatology* **47**, 321–331 (2008).
4. Liang, T. J. & Ghany, M. G. Current and future therapies for hepatitis C virus infection. *N. Engl. J. Med.* **368**, 1907–1917 (2013).
5. Liang, T. J. & Ghany, M. G. Therapy of hepatitis C—back to the future. *N. Engl. J. Med* **370**, 2043–2047 (2014).
6. Ward, J. W. & Hinman, A. R. What is needed to eliminate hepatitis B virus and hepatitis C virus as global health threats. *Gastroenterology* **156**, 297–310 (2019).
7. Zeuzem, S. et al. Sofosbuvir and ribavirin in HCV genotypes 2 and 3. *N. Engl. J. Med* **370**, 1993–2001 (2014).
8. Fourati, S. et al. Frequent antiviral treatment failures in patients infected with hepatitis C virus genotype 4, subtype 4r. *Hepatology* **69**, 513–523 (2019).
9. Childs, K. et al. Suboptimal SVR rates in African patients with atypical genotype 1 subtypes: implications for global elimination of hepatitis C. *J. Hepatol.* **71**, 1099–1105 (2019).
10. Wei, L. et al. Sofosbuvir–velpatasvir for treatment of chronic hepatitis C virus infection in Asia: a single-arm, open-label, phase 3 trial. *Lancet Gastroenterol. Hepatol.* **4**, 127–134 (2019).
11. Garrison, K. L., German, P., Mogalian, E. & Mathias, A. The drug–drug interaction potential of antiviral agents for the treatment of chronic hepatitis C infection. *Drug Metab. Dispos.* **46**, 1212–1225 (2018).
12. Voelker, R. The 8-week cure for hepatitis C. *JAMA* **318**, 996 (2017).
13. Pawlotsky, J.-M. Hepatitis C virus resistance to direct-acting antiviral drugs in interferon-free regimens. *Gastroenterology* **151**, 70–86 (2016).
14. Kurosaki, M. et al. Nation-wide real world study of NS5A resistance-associated substitutions in patients who failed prior daclatasvir plus asunaprevir: identification of specific pattern that impacts re-treatment outcome by ledipasvir/sofosbuvir. *Hepatology* **68**, abstr. 200 (2018).
15. Di Maio, V. C. et al. Frequent NS5A and multiclass resistance in almost all HCV genotypes at DAA failures: what are the chances for second-line regimens? *J. Hepatol.* **68**, 597–600 (2018).
16. Howe, A. et al. A real world resistance profile of virologic failures collected from an international collaboration (SHARED). *Hepatology* **68**, abstr. 204 (2018).
17. Teegen, E. M., Maurer, M. M., Globke, B., Pratschke, J. & Eurich, D. Liver transplantation for hepatitis-B-associated liver disease—three decades of experience. *Transpl. Infect. Dis.* **21**, e12997 (2019).
18. Hu, Z. et al. Novel cell-based hepatitis C virus infection assay for quantitative high-throughput screening of anti-hepatitis C virus compounds. *Antimicrob. Agents Chemother.* **58**, 995–1004 (2014).
19. He, S. et al. Development of an aryloxazole class of hepatitis C virus inhibitors targeting the entry stage of the viral replication cycle. *J. Med. Chem.* **60**, 6364–6383 (2017).
20. He, S. et al. Repurposing of the antihistamine chlorcyclizine and related compounds for treatment of hepatitis C virus infection. *Sci. Transl. Med.* **7**, 282ra249 (2015).
21. Tscherne, D. M. et al. Time- and temperature-dependent activation of hepatitis C virus for low-pH-triggered entry. *J. Virol.* **80**, 1734–1741 (2006).

22. Ashfaq, U. A., Javed, T., Rehman, S., Nawaz, Z. & Riazuddin, S. Lysosomotropic agents as HCV entry inhibitors. *Virol. J.* **8**, 163 (2011).
23. Sharma, N. R. et al. Hepatitis C virus is primed by CD81 protein for low pH-dependent fusion. *J. Biol. Chem.* **286**, 30361–30376 (2011).
24. Bush, C. O. et al. A small-molecule inhibitor of hepatitis C virus infectivity. *Antimicrob. Agents Chemother.* **58**, 386–396 (2014).
25. Zhou, N. et al. Characterization of NS5A polymorphisms and their impact on response rates in patients with HCV genotype 2 treated with daclatasvir-based regimens. *J. Antimicrob. Chemother.* **71**, 3495–3505 (2016).
26. Gottwein, J. M. et al. Development and characterization of hepatitis C virus genotype 1–7 cell culture systems: role of CD81 and scavenger receptor class B type I and effect of antiviral drugs. *Hepatology* **49**, 364–377 (2009).
27. Lin, B., He, S., Yim, H. J., Liang, T. J. & Hu, Z. Evaluation of antiviral drug synergy in an infectious HCV system. *Antivir. Ther.* **21**, 595–603 (2016).
28. Bijnsdorp, I. V., Giovannetti, E. & Peters, G. J. in *Cancer Cell Culture: Methods and Protocols* (ed. Cree, I. A.) 421–434 (Springer Science+Business Media, 2011).
29. Prichard, M. N. & Shipman, C.Jr. A three-dimensional model to analyze drug-drug interactions. *Antivir. Res.* **14**, 181–205 (1990).
30. Puoti, M. et al. High SVR12 with 8-week and 12-week glecaprevir/pibrentasvir therapy: an integrated analysis of HCV genotype 1–6 patients without cirrhosis. *J. Hepatol.* **69**, 293–300 (2018).
31. Ng, T. I. et al. In vitro antiviral activity and resistance profile of the next-generation hepatitis C virus NS3/4A protease inhibitor glecaprevir. *Antimicrob. Agents Chemother.* **62**, e01620-17 (2017).
32. Ng, T. I. et al. In vitro antiviral activity and resistance profile of the next-generation hepatitis C virus NS5A inhibitor pibrentasvir. *Antimicrob. Agents Chemother.* **61**, e02558-16 (2017).
33. Osawa, M. et al. Real-world efficacy of glecaprevir plus pibrentasvir for chronic hepatitis C patient with previous direct-acting antiviral therapy failures. *J. Gastroenterol.* **54**, 291–296 (2019).
34. Osawa, M. et al. Efficacy of glecaprevir and pibrentasvir treatment for genotype 1b hepatitis C virus drug resistance-associated variants in humanized mice. *J. Gen. Virol.* **100**, 1123–1131 (2019).
35. Krishnan, P. et al. Pooled resistance analysis in patients with hepatitis C virus genotype 1 to 6 infection treated with glecaprevir-pibrentasvir in phase 2 and 3 clinical trials. *Antimicrob. Agents Chemother.* **62**, e01249-18 (2018).
36. Li, H. F., Huang, C.-H., Ai, L.-S., Chuang, C.-K. & Chen, S. S. L. Mutagenesis of the fusion peptide-like domain of hepatitis C virus E1 glycoprotein: involvement in cell fusion and virus entry. *J. Biomed. Sci.* **16**, 89 (2009).
37. Tong, Y., Lavillette, D., Li, Q. & Zhong, J. Role of hepatitis C virus envelope glycoprotein E1 in virus entry and assembly. *Front. Immunol.* **9**, 1411 (2018).
38. Hu, Z. et al. Chlorcyclizine inhibits viral fusion of hepatitis C virus entry by directly targeting HCV envelope glycoprotein 1. *Cell Chem. Biol.* **27**, 780–792 (2020).
39. Cocquerel, L., Wychowski, C., Minner, F., Penin, F. & Dubuisson, J. Charged residues in the transmembrane domains of hepatitis C virus glycoproteins play a major role in the processing, subcellular localization, and assembly of these envelope proteins. *J. Virol.* **74**, 3623–3633 (2000).
40. Freedman, H. et al. Computational prediction of the heterodimeric and higher-order structure of gpE1/gpE2 envelope glycoproteins encoded by hepatitis C virus. *J. Virol.* **91**, e02309-16 (2017).
41. Partridge, A. W., Therien, A. G. & Deber, C. M. Missense mutations in transmembrane domains of proteins: phenotypic propensity of polar residues for human disease. *Proteins* **54**, 648–656 (2004).
42. Kong, L. et al. Hepatitis C virus E2 envelope glycoprotein core structure. *Science* **342**, 1090–1094 (2013).
43. Serre, S. B. N., Krarup, H. B., Bukh, J. & Gottwein, J. M. Identification of alpha interferon-induced envelope mutations of hepatitis C virus in vitro associated with increased viral fitness and interferon resistance. *J. Virol.* **87**, 12776–12793 (2013).
44. Bogomolov, P. et al. Treatment of chronic hepatitis D with the entry inhibitor myrcludex B: first results of a phase Ib/IIa study. *J. Hepatol.* **65**, 490–498 (2016).
45. Bethea, E. D. et al. Pre-emptive pangenotypic direct acting antiviral therapy in donor HCV-positive to recipient HCV-negative heart transplantation: an open-label study. *Lancet Gastroenterol. Hepatol.* **4**, 771–780 (2019).
46. Woolley, A. E. et al. Heart and lung transplants from HCV-infected donors to uninfected recipients. *N. Engl. J. Med.* **380**, 1606–1617 (2019).
47. Rolt, A. et al. Preclinical pharmacological development of chlorcyclizine derivatives for the treatment of hepatitis C virus infection. *J. Infect. Dis.* **217**, 1761–1769 (2018).
48. Perin, P. M. et al. Flunarizine prevents hepatitis C virus membrane fusion in a genotype-dependent manner by targeting the potential fusion peptide within E1. *Hepatology* **63**, 49–62 (2016).
49. Vausselin, T. et al. Identification of a new benzimidazole derivative as an antiviral against hepatitis C virus. *J. Virol.* **90**, 8422–8434 (2016).
50. Harrison, S. C. Viral membrane fusion. *Virology* **479–480**, 498–507 (2015).
51. Rybak, J.-N., Scheurer, S. B., Neri, D. & Elia, G. Purification of biotinylated proteins on streptavidin resin: a protocol for quantitative elution. *Proteomics* **4**, 2296–2299 (2004).

Acknowledgements

This work was supported by the Intramural Research Program of the National Institute of Diabetes and Digestive and Kidney Diseases and National Center for Advancing Translational Sciences, NIH, the Molecular Libraries Initiative funding to the University of Kansas Specialized Chemistry Center (grant no. U54HG005031) and the Japan Agency for Medical Research and Development (grant no. JP18fk0210020h0002).

Author contributions

T.J.L., C.D.M., Z.H. and K.J.F. conceptualized and designed the study. C.D.M., M.I., D.C.T., A.R., X.X., A.Q.W., D.L., T.U., M.O., Y.T., K.L., X.H., S.B.P., N.C., P.H.I., A.E.D., N.S., J.J.M., Z.H., K.C. and K.J.F. performed, analysed and contributed to all the experiments. C.D.M., Z.H. and T.J.L. wrote the manuscript. All other authors reviewed and contributed to the manuscript.

Competing interests

The authors declare no competing interests.

Additional information

Extended data is available for this paper at https://doi.org/10.1038/s41564-020-0781-2.

Supplementary information is available for this paper at https://doi.org/10.1038/s41564-020-0781-2.

Correspondence and requests for materials should be addressed to T.J.L.

Peer review information Peer reviewer reports are available.

Reprints and permissions information is available at www.nature.com/reprints.

Publisher's note Springer Nature remains neutral with regard to jurisdictional claims in published maps and institutional affiliations.

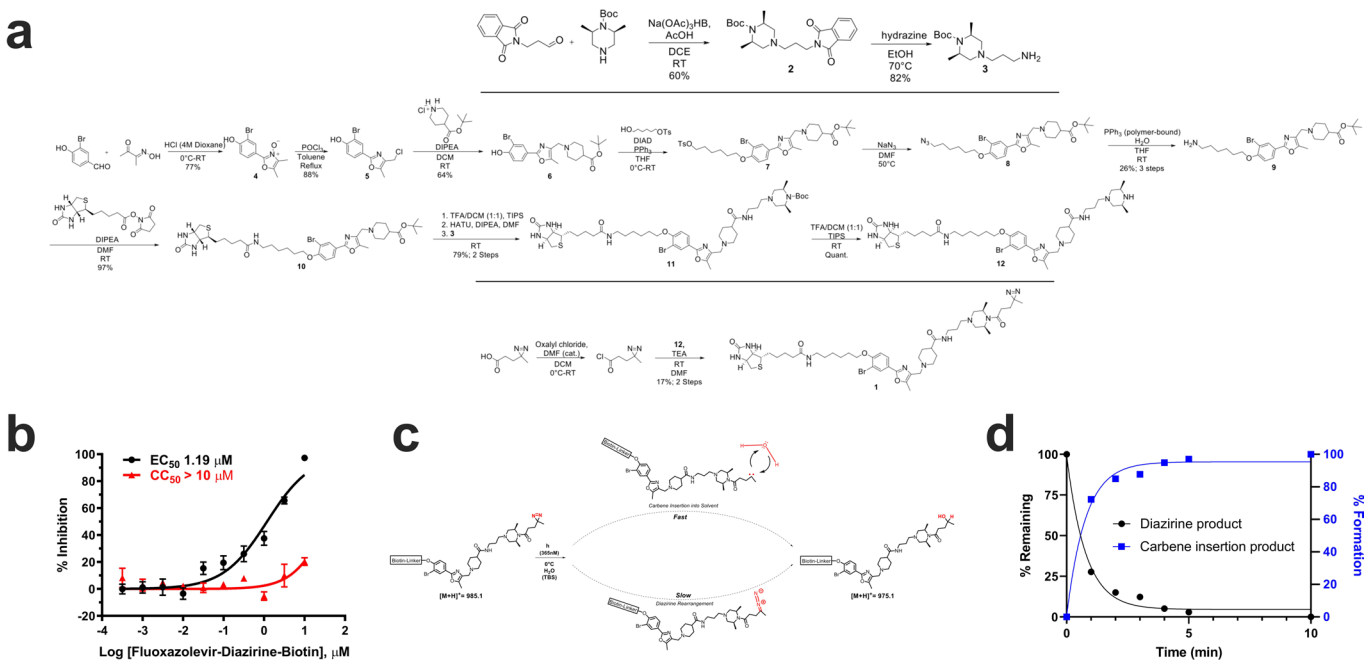

Extended Data Fig. 1 | Synthesis, efficacy, and photolysis of the fluoxazolevir-diazirine-biotin probe. a, The general synthetic scheme of the fluoxazolevir-diazirine-biotin (fluoxazolevir-DB) probe is shown. Each intermediate was confirmed with ^{1}H NMR and LCMS. See supplemental document for more information on each synthetic step. **b**, Fluoxazolevir-DB probe retains anti-HCV activity *in vitro* and shows inhibition against HCV infection in a dose-dependent manner. Data are presented as mean values ± SEM of 6 biologically independent replicates. **c**, The degradation of fluoxazolevir-DB via UV irradiation is shown. **d**, The fluoxazolevir-DB was exposed to UV irradiation with a 100 W mercury lamp with a 365 nm bypass filter. Disappearance of fluoxazolevir-DB was measured over time via LCMS and underwent a complete conversion to the carbene insertion product within 10 min. All results are representative of three independent experiments.

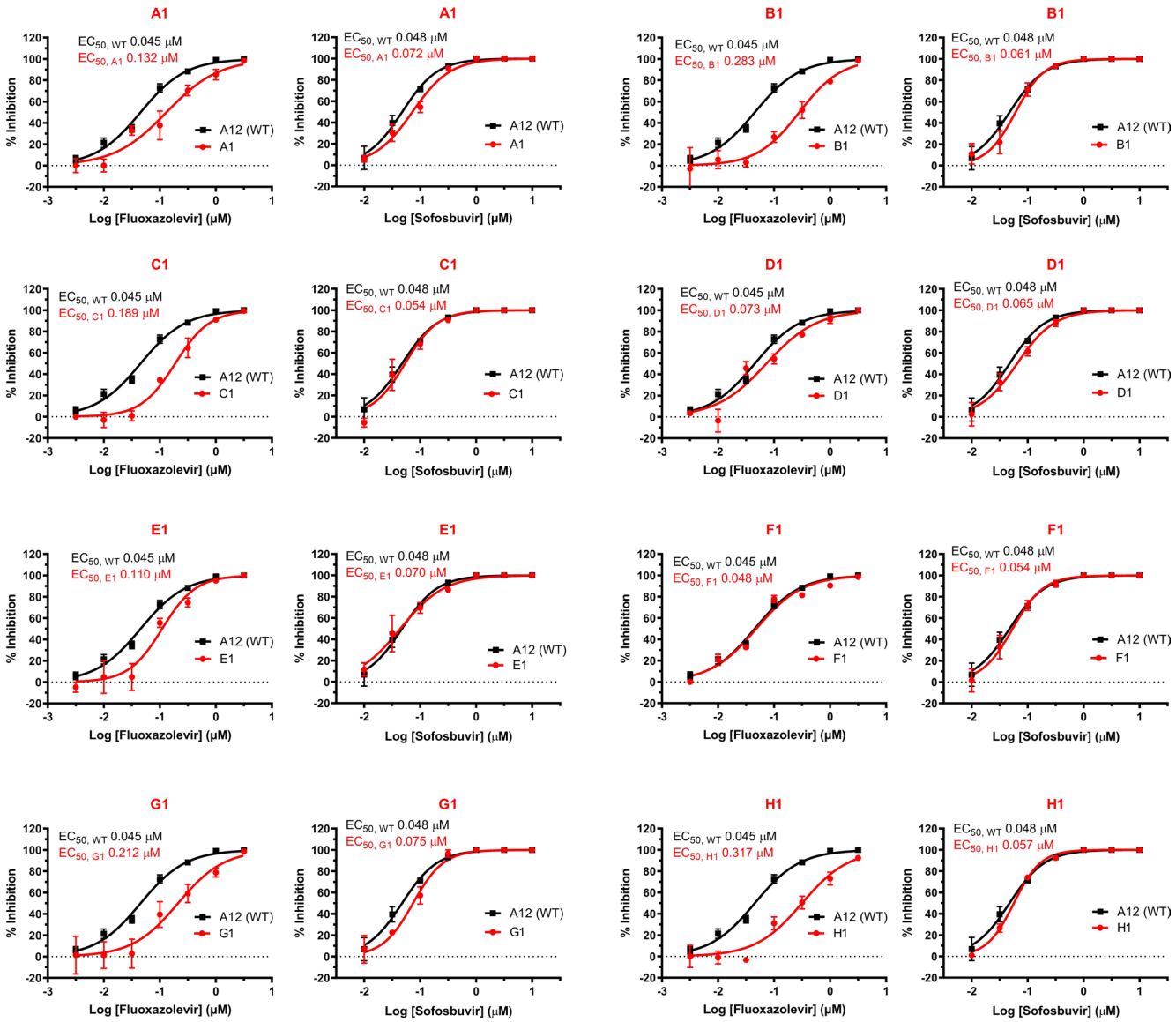

Extended Data Fig. 2 | Dose-response curves of fluoxazolevir against amplified HCV from the *in vitro* drug resistance selection assay. Among the 8 serial passages with potential RAS-containing HCV generated from the drug resistance selection assay (Fig. 2a), the viruses in the following wells (and their identified mutations) showed moderate resistance with EC_{50} values increasing by at least two-fold comparing to the wild-type control: A1 (F291L, V414A), B1 (I374T), C1 (D382E, T395A, M405V, P616A), E1 (F291V), G1 (A274S) and H1 (M267V, V284A). The same viruses were tested against sofosbuvir as a control and were equally sensitive to sofosbuvir as the wild type virus. Data are presented as mean values ± SEM of 3 biologically independent replicates. All results are representative of three independent experiments.

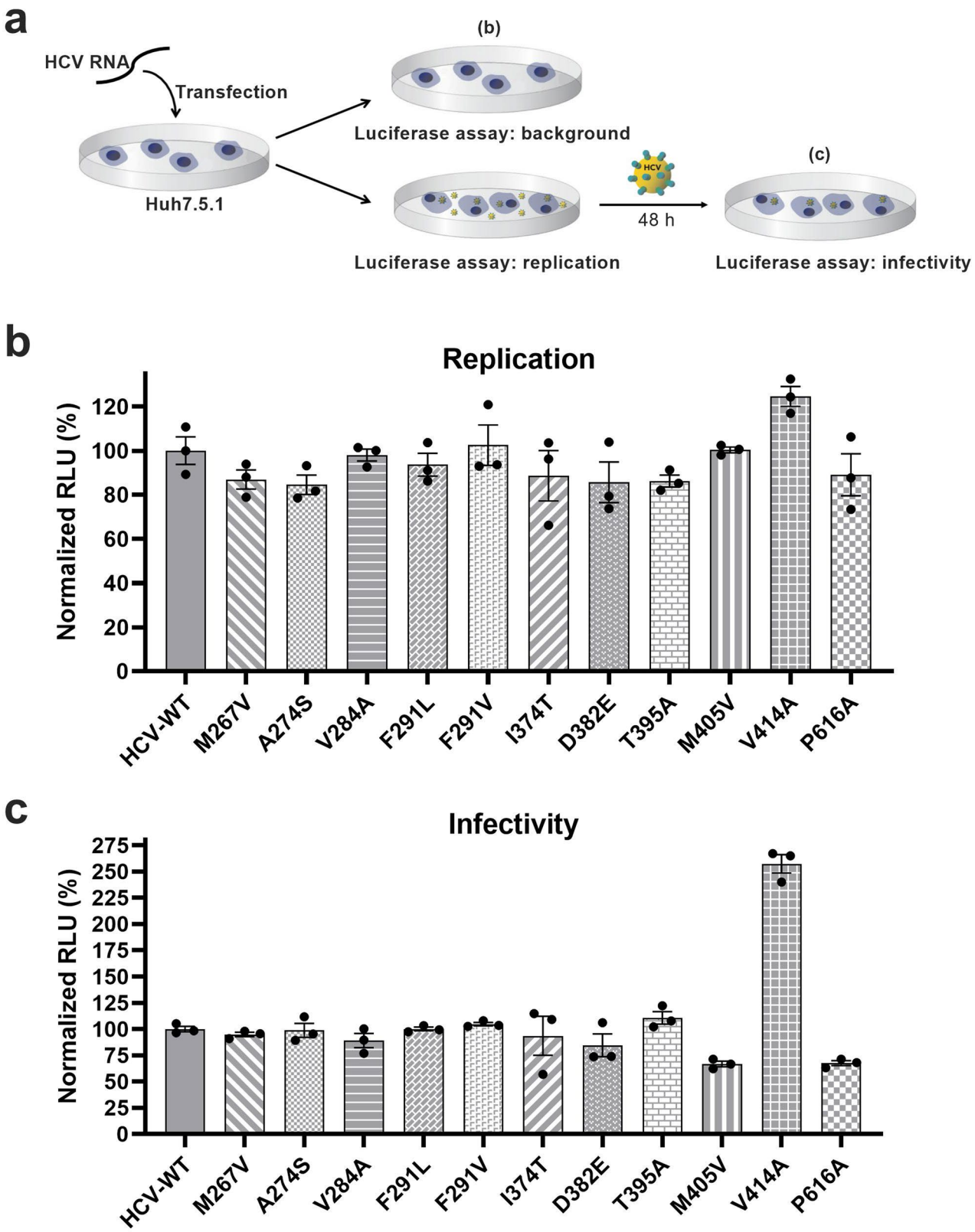

Extended Data Fig. 3 | Viral fitness of the generated RAS-containing HCV. a, The viral fitness assay scheme is shown here. Huh7.5.1 cells were electroporated with the RNA of each HCV RAS-RLuc construct. **b**, The first part of the assay assesses the replication capacity for each RAS-containing HCV. Luminescence was measured 4 h and 3 days after electroporation and the readings obtained 4 h after electroporation was used as background. **c**, The second part of the assay assesses infectivity of each RAS. Viral medium harvested 3 days after electroporation from part b was used to reinfect 10^4 naïve Huh7.5.1 cells in a 96-well plate. Luminescence was measured 48 h after reinfection and all measurements were normalized to HCV-WT. Data are presented as mean values ± SEM of 3 biologically independent replicates. All results are representative of three independent experiments.

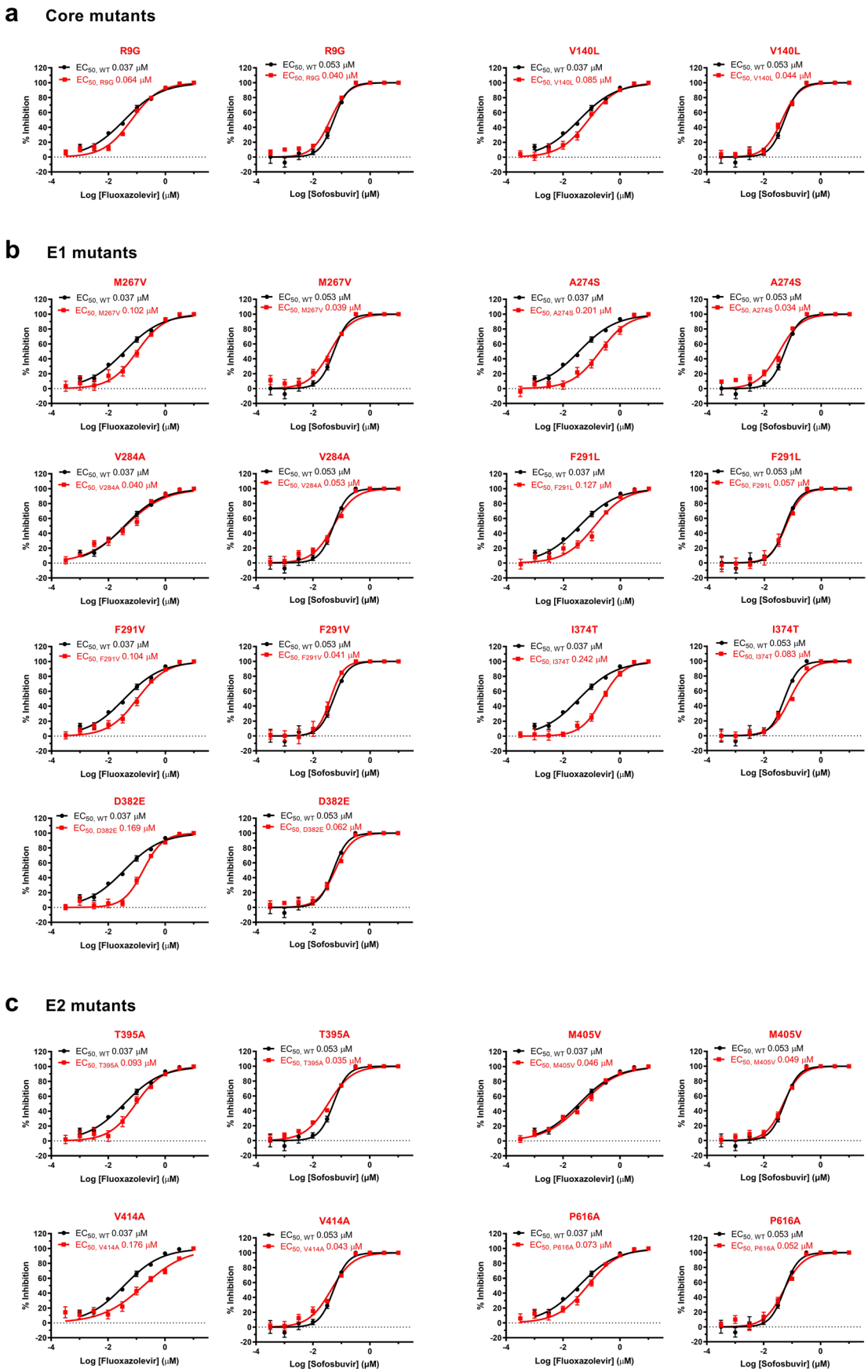

Extended Data Fig. 4 | See next page for caption.

Extended Data Fig. 4 | Dose-response curves of fluoxazolevir against HCV mutants with putative RASs in core, E1 and E2 regions. Huh7.5.1 cells in 96-well plates were infected with wild-type HCV-RLuc (GT 2a) and HCV-RLuc mutants with various putative RASs (R9G, V140L, M267V, A274S, V284A, F291L, F291V, I374T, D382E, T395A, M405V, V414A and P616A) in the presence of various fluoxazolevir concentrations as indicated. Cells were harvested 48 h after infection and luminescence assessed via the luciferase assay. The EC_{50} values for wild-type HCV-RLuc (black circles) and the HCV mutants (red squares) were calculated with Prism 7. Data are presented as mean values ± SEM of 8 biologically independent replicates. All results are representative of three independent experiments.

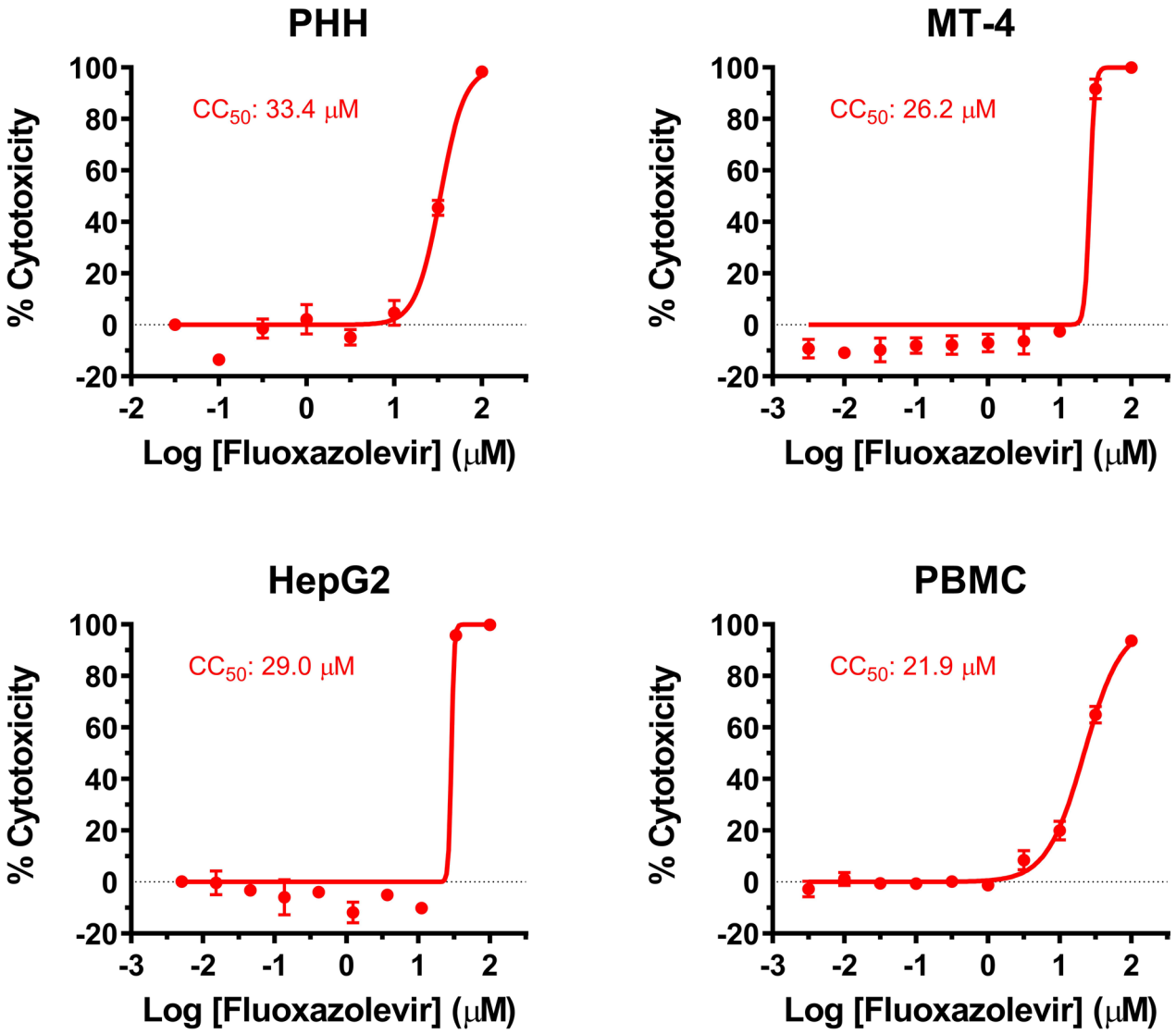

Extended Data Fig. 5 | Cytotoxicity of fluoxazolevir against primary human hepatocytes, HepG2 cells, MT-4 cells and peripheral blood mononuclear cells. Cells were treated with fluoxazolevir for 3 days and processed for the ATPlite cytotoxicity assay. CC_{50} values were calculated with the software, Prism 7. Data are presented as mean values ± SEM of 3 biologically independent replicates. All results are representative of three independent experiments.

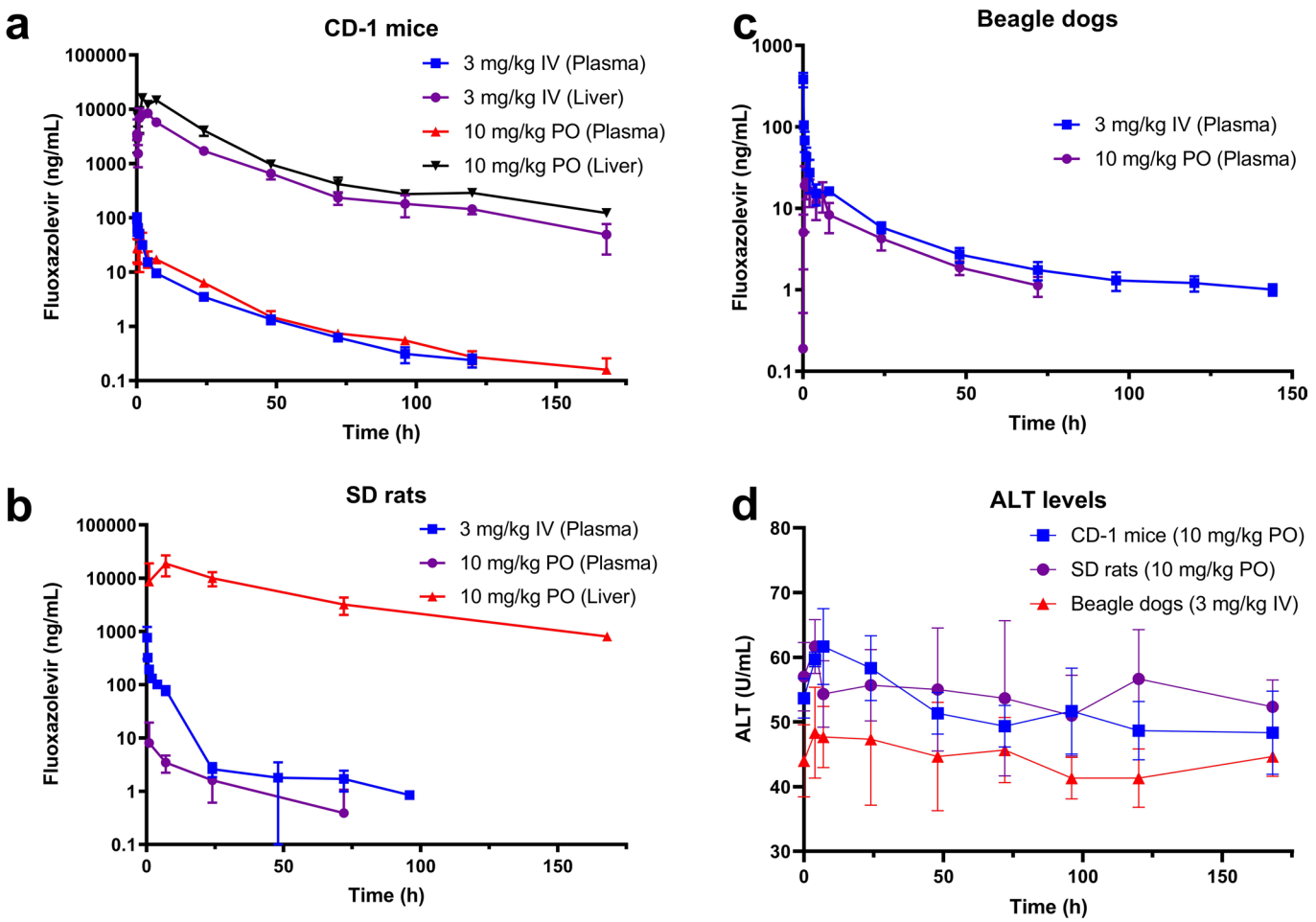

Extended Data Fig. 6 | Pharmacokinetics of fluoxazolevir. Pharmacokinetic studies of fluoxazolevir were performed in (**a**) male CD-1 mouse, (**b**) male SD rat and (**c**) male beagle dog models (n = 3 animals). The concentration profiles of fluoxazolevir were measured after either a single PO dose of 10 mg/kg or a single IV dose of 3 mg/kg. Compound concentrations were measured by UPLC-MS/MS. **d**, Serum alanine aminotransferase (ALT) levels were measured in each animal model to assess the potential toxicity of fluoxazolevir *in vivo*. For CD-1 mice and SD rats, ALTs from the 10 mg/kg PO groups were shown, and for beagle dogs, the 3 mg/kg IV group was shown. Data are presented as mean values ± standard deviations.

Animal	CD-1 Mouse[1] (n = 39)						SD Rat[1] (n = 15)	
Dose	PO (10 mg/kg)		PO (5 mg/kg)				PO (10 mg/kg)	
Sample	plasma	liver	plasma	liver	brain	heart	Plasma	Liver
$AUC_{0-\infty}$[2] (μM•h)	1.15	754	0.419	389	3.23	39.7	0.300	1870
$t_{1/2}$[2] (h)	37	45	27	26	58	32	21	37
T_{max}[2] (h)	2	2	1	7	7	24	1	7
C_{max}[2] (μM)	0.084	34.4	0.031	13.8	0.042	0.78	0.017	39.9
AUC ratio (Tissue/Plasma)	-	659	-	929	7.7	95	-	6250

Extended Data Fig. 7 | Tissue distribution of fluoxazolevir after PO administration in rodents. [1]The plasma and tissue concentrations of fluoxazolevir were measured after a single PO dose of fluoxazolevir. Thirty-nine mice and fifteen rats ($n = 3$/time point) for tissue collection. [2] $AUC_{0-\infty}$: area under the curve from zero to infinity; $t_{1/2}$: half-life; T_{max}: time to reach the maximal concentration; C_{max}: maximal concentration after PO administration.

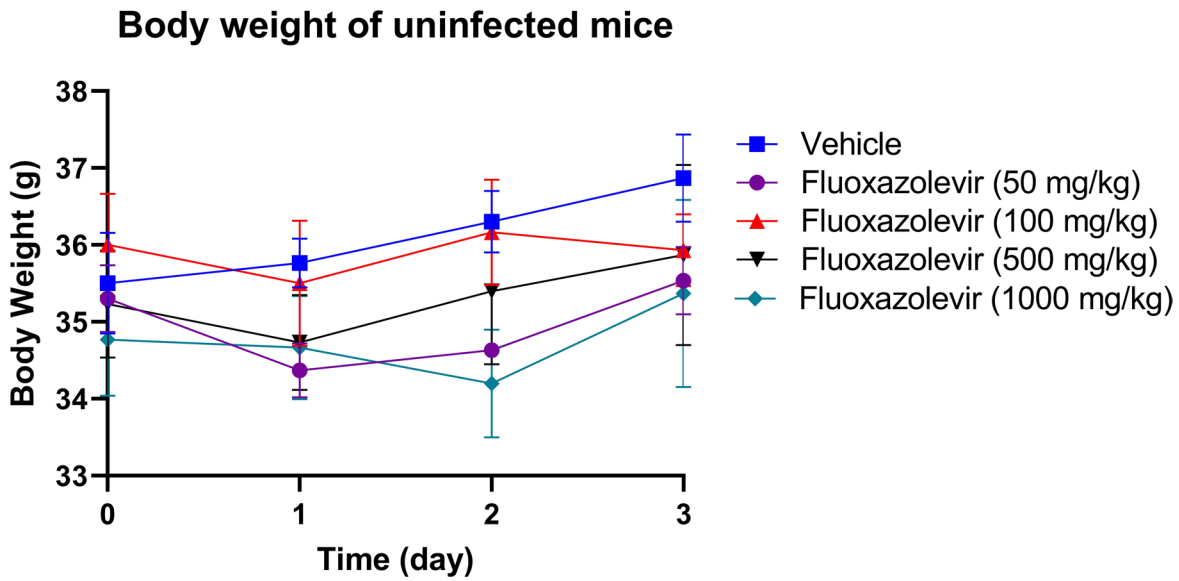

Extended Data Fig. 8 | Maximal tolerable dose of fluoxazolevir in mice. The study was performed by Pharmaron Inc. (Beijing, PR China). Single doses of fluoxazolevir (50 mg/kg, 100 mg/kg, 500 mg/kg and 1000 mg/kg) were administered via oral gavage to CD-1 mice (n = 3 mice per group) and observed for 3 days. Body weights of all animals were recorded daily. All study animals were monitored behavior such as respite, food and water consumption (by cage side checking), circling, eye/hair matting and any other abnormal effect. Any mortality and/or abnormal clinical signs were recorded. All animals were sacrificed for necropsy on day 3. Data are presented as mean values ± SEM.

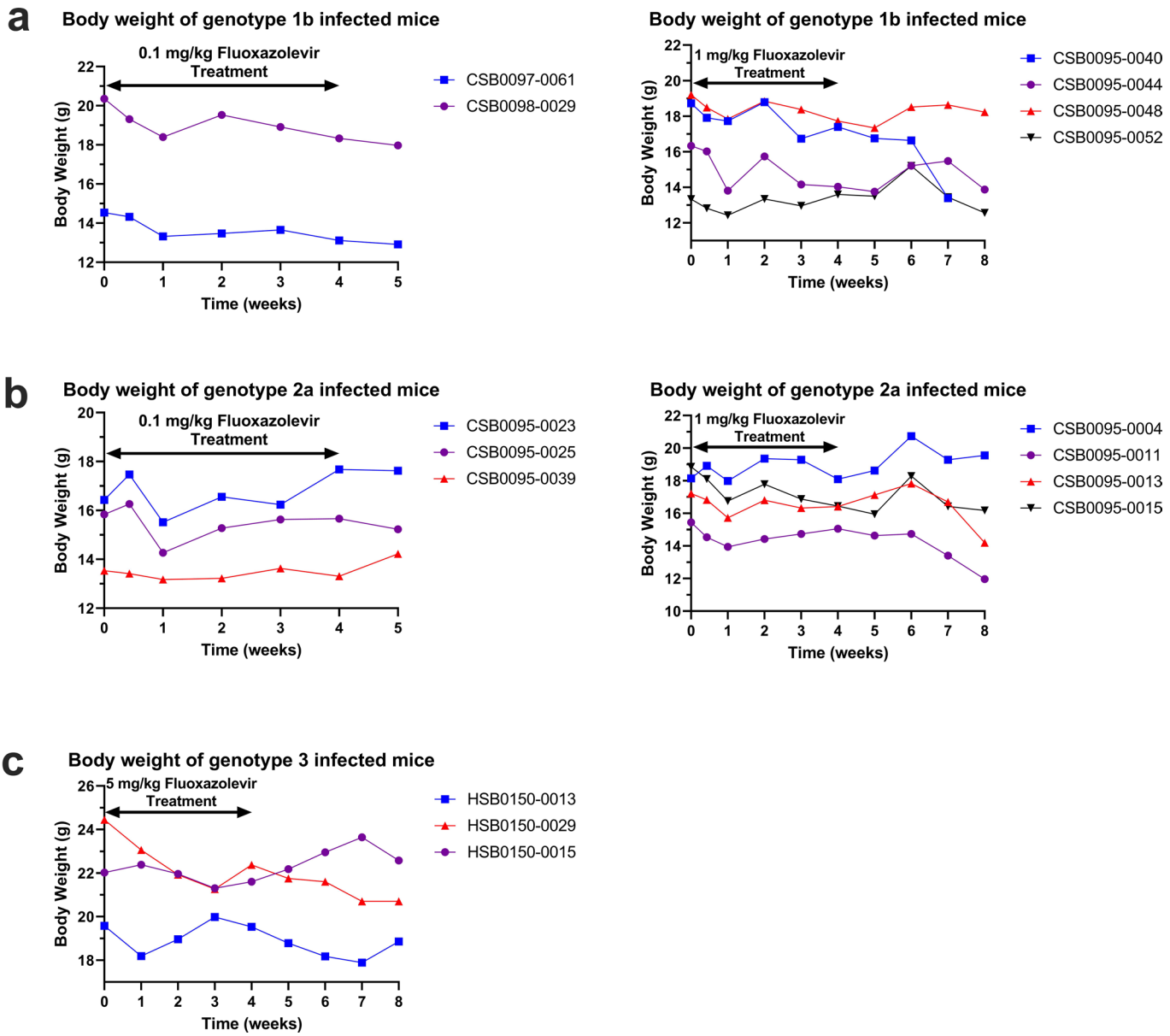

Extended Data Fig. 9 | Lack of toxicity of fluoxazolevir monotherapy in genotypes 1b, 2a and 3-infected *Alb-uPA/Scid* mice. The body weights of the humanized *Alb-uPA/Scid* mice infected with HCV genotypes **(a)** 1b (n = 2-4 mice), **(b)** 2a (n = 3-4 mice) and **(c)** 3 (n = 3 mice) were monitored during and after fluoxazolevir treatment as described in Fig. 4a, b, Supplementary Figure 3–5. All mice in each group were weighed regularly for evidence of toxicity.

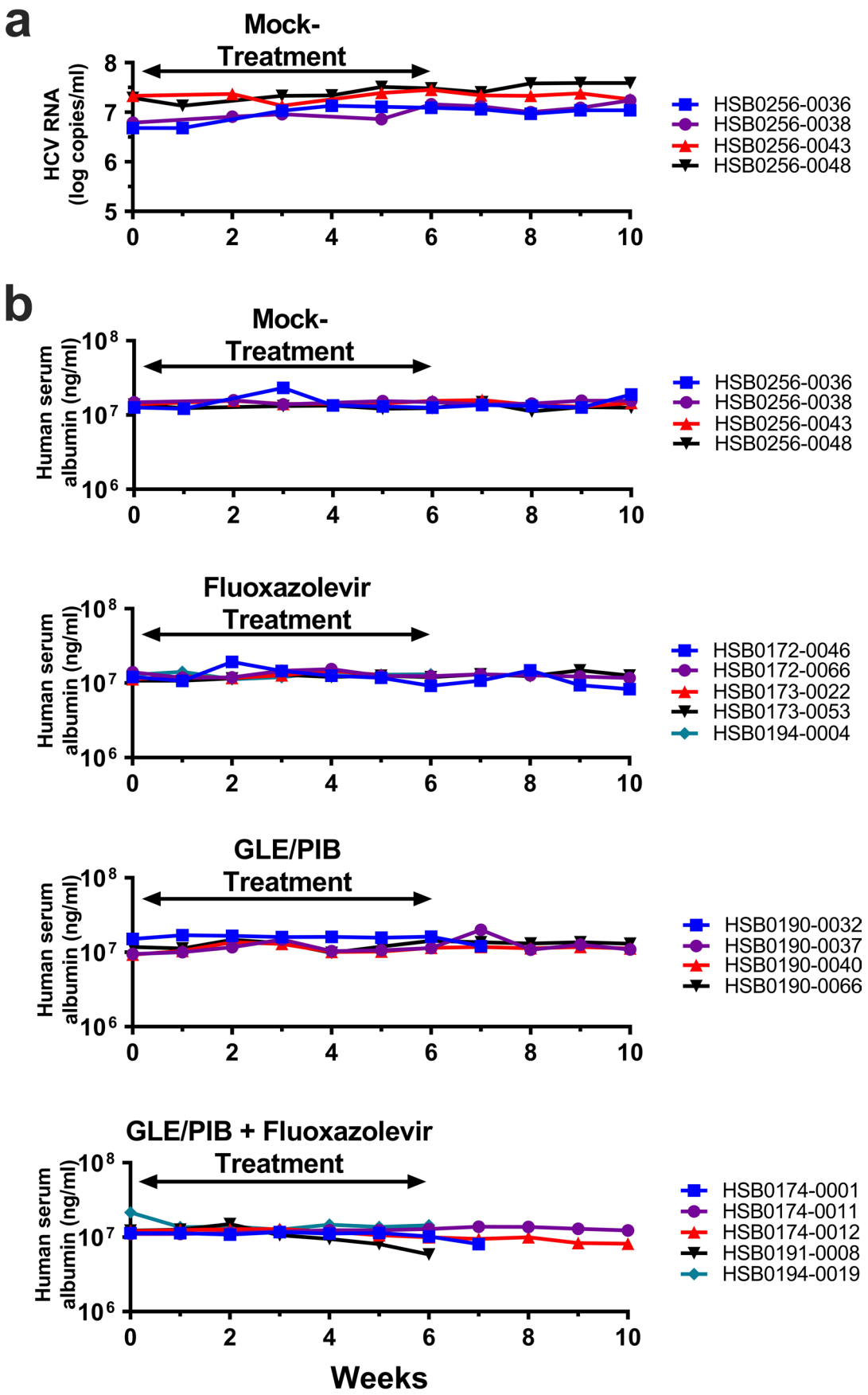

Extended Data Fig. 10 | See next page for caption.

Extended Data Fig. 10 | HCV RNA and serum human albumin levels of mice infected with multidrug-resistant HCV. Humanized *Alb-uPA/Scid* mice were infected with the multidrug-resistant HCV strain and were either untreated (n = 4 mice) or treated with fluoxazolevir (n = 5 mice), GLE/PIB (n = 4 mice) or combination (n = 5 mice). Serum HCV RNA and human serum albumin levels were monitored weekly. **a**, Serum HCV RNA levels of untreated humanized *Alb-uPA/Scid* mice showed steady levels during follow-up. Time 0 is comparable to the time of initiation of treatment in (b). Mouse serum samples at the end of the 20 weeks were sequenced and the same NS3 and NS5a mutations as the inoculum virus were identified. **b**, Human serum albumin levels of untreated mice and mice treated with fluoxazolevir (5 mg/kg), glecaprevir (60 mg/kg) and pibrentasvir (24 mg/kg). Weekly serum levels of human albumin of individual mice were plotted. Weekly HCV RNA measurements of individual mice for each time point are shown in Fig. 4c. Serum human albumin graphs that end before the 10 weeks are due to death of the mice.

nature research

Corresponding author(s): T. Jake Liang

Last updated by author(s): June 27, 2020

Reporting Summary

Nature Research wishes to improve the reproducibility of the work that we publish. This form provides structure for consistency and transparency in reporting. For further information on Nature Research policies, see Authors & Referees and the Editorial Policy Checklist.

Statistics

For all statistical analyses, confirm that the following items are present in the figure legend, table legend, main text, or Methods section.

n/a	Confirmed
☐	☒ The exact sample size (*n*) for each experimental group/condition, given as a discrete number and unit of measurement
☐	☒ A statement on whether measurements were taken from distinct samples or whether the same sample was measured repeatedly
☐	☒ The statistical test(s) used AND whether they are one- or two-sided *Only common tests should be described solely by name; describe more complex techniques in the Methods section.*
☒	☐ A description of all covariates tested
☒	☐ A description of any assumptions or corrections, such as tests of normality and adjustment for multiple comparisons
☐	☒ A full description of the statistical parameters including central tendency (e.g. means) or other basic estimates (e.g. regression coefficient) AND variation (e.g. standard deviation) or associated estimates of uncertainty (e.g. confidence intervals)
☐	☒ For null hypothesis testing, the test statistic (e.g. *F*, *t*, *r*) with confidence intervals, effect sizes, degrees of freedom and *P* value noted *Give P values as exact values whenever suitable.*
☒	☐ For Bayesian analysis, information on the choice of priors and Markov chain Monte Carlo settings
☒	☐ For hierarchical and complex designs, identification of the appropriate level for tests and full reporting of outcomes
☒	☐ Estimates of effect sizes (e.g. Cohen's *d*, Pearson's *r*), indicating how they were calculated

Our web collection on statistics for biologists contains articles on many of the points above.

Software and code

Policy information about availability of computer code

Data collection	The software program, Omega (Software Version: 1.10; Firmware Version: 1.21), was used to measure luminescence readings for all Renilla luciferase assays. All NMR spectra have been analyzed with the software, MestReNova (Software Version:12.0.0).
Data analysis	The software program, Prism 7 for Mac OS X (Version 7.0d), was used to analyze all assays and used to determine statistical significance. T tests and two-sided P values were used in all analyses. The softwares, CalcuSyn (Version 2.11) and MacSynergy II (Version 1.0), were also used to analyze the synergy experiments. CalcuSyn uses combination indices near the EC50 values of each drug to determine synergism/antagonism. The softwares, MAFFT version 7 and Berkeley WebLogo (Version 2.8.2), were used to generate sequence alignments.

For manuscripts utilizing custom algorithms or software that are central to the research but not yet described in published literature, software must be made available to editors/reviewers. We strongly encourage code deposition in a community repository (e.g. GitHub). See the Nature Research guidelines for submitting code & software for further information.

Data

Policy information about availability of data

All manuscripts must include a data availability statement. This statement should provide the following information, where applicable:

- Accession codes, unique identifiers, or web links for publicly available datasets
- A list of figures that have associated raw data
- A description of any restrictions on data availability

The data that was used to generate the HCV E1 protein alignment (genotypes 1-6) and to support the findings of this study are available from the Virus Pathogen Database (https://www.viprbrc.org/brc/home.spg?decorator=flavi_hcv). The genotype 7 protein sequence data that support the findings of this study have been deposited in NCBI with the following accession codes: YP_009272536, ARB18146. All other data that support the findings of this study are available from the corresponding author upon reasonable request.

Field-specific reporting

Please select the one below that is the best fit for your research. If you are not sure, read the appropriate sections before making your selection.

☒ Life sciences ☐ Behavioural & social sciences ☐ Ecological, evolutionary & environmental sciences

For a reference copy of the document with all sections, see nature.com/documents/nr-reporting-summary-flat.pdf

Life sciences study design

All studies must disclose on these points even when the disclosure is negative.

Sample size	To assess statistical significance, sample sizes were set to at least three. For all our in vitro assays, at least 6 replicates were generated to obtain accurate means and errors. At least three species were used for each experiment in our in vivo studies to obtain reliable means and errors. All animals were selected randomly and no animals were given preferential treatment when allocating them into the experimental groups. The sample size was chosen based on the minimal number needed for statistical analysis. Limitations in cost, unforeseen events (e.g., animal death), and established protocols prevented us from having a greater number of replicates for the in vivo studies.
Data exclusions	Data measurements that were considered to be outliers were excluded. In the in vitro portion of this study, data points were removed if they are certainly related to human error or if data could not be replicated. In the in vivo portion of the study, data exclusion occurred when the humanized chimeric mice died too early in the study. If these outliers were not excluded, then inaccurate conclusions could be made.
Replication	All in vitro experiments were repeated at least three times to ensure consistency and reproducibility. All attempts at replication were successful for the in vitro experiments. In the in vivo studies, at least 3 animals were used for each group. Limitations in cost, unforeseen events, and established protocols prevented us from replicating in vivo experiments.
Randomization	All mice, rats and dogs used in the pharmacokinetics or in vivo efficacy studies were selected randomly. Animals were not given any preferential treatment when randomly allocating them into control or experimental groups. Randomization in our in vitro experiments was not relevant and did not apply to our study. We looked into the effects of one particular drug so the in vitro experiments could not be randomized.
Blinding	Blinding was not possible in this study since humans or any other subjective species were not utilized in any of the experiments. The investigator was not blinded during data collection and analysis because s/he was not subjected to any bias or ambiguity. The study looked into the effects of one particular drug and could not be blinded.

Reporting for specific materials, systems and methods

We require information from authors about some types of materials, experimental systems and methods used in many studies. Here, indicate whether each material, system or method listed is relevant to your study. If you are not sure if a list item applies to your research, read the appropriate section before selecting a response.

Materials & experimental systems

n/a	Involved in the study
☐	☒ Antibodies
☐	☒ Eukaryotic cell lines
☒	☐ Palaeontology
☐	☒ Animals and other organisms
☒	☐ Human research participants
☒	☐ Clinical data

Methods

n/a	Involved in the study
☒	☐ ChIP-seq
☒	☐ Flow cytometry
☒	☐ MRI-based neuroimaging

Antibodies

Antibodies used	The antibodies used in immunofluorescence were: Anti-HCV core monoclonal antibody was generated from a 6G7 hybridoma clone and was provided by Drs. Harry Greenberg and Xiaosong He, Stanford University. Invitrogen AlexaFluor488 goat anti-mouse IgG (H+L) Cross-Adsorbed Manufacturer: Invitrogen; Catalog #: A11001; Lot #: 1907294
Validation	The specificity of the anti-HCV core antibody was validated through an immunoblot screening using a core peptide antigen. In the presence of the core antibody, HCV infected cells were positively stained. Uninfected cells were negatively stained.

Eukaryotic cell lines

Policy information about cell lines

Cell line source(s)	Huh7.5.1 is a derivative of Huh7 cells. More information on Huh7 cells can be found at the Japanese Collection of Research Bioresources (JCRB #: JCRB0403). HepG2 cells and MT-4 cells were obtained from ATCC. Primary human hepatocytes were obtained from ThermoFisher Scientific.
Authentication	None of the cell lines used were authenticated, but they all behaved as expected.
Mycoplasma contamination	All cell lines were tested for mycoplasma contamination and all tests were negative.
Commonly misidentified lines (See ICLAC register)	No commonly mis-identified lines were used in this study.

Animals and other organisms

Policy information about studies involving animals; ARRIVE guidelines recommended for reporting animal research

Laboratory animals	Male Alb-uPA/Scid mice (age 4 weeks), male CD-1 mice (age 4 months), male Sprague Dawley rats (age 6 months) and male beagle dogs (age 4-7 years) were used in this study.
Wild animals	Wild animals were not involved in this study.
Field-collected samples	The study did not involved field-collected samples.
Ethics oversight	All male CD-1 mice and SD rats were maintained at the NIH animal facilities where all protocols were followed by the Division of Veterinary Resources and the Animal Care and Use Committee at the NIH. The male beagle dogs were conducted by the Charles River Laboratories in Worcester, MA under their IACUC approved protocol (PS-0002-DA-DE). Alb-uPA/Scid mice were maintained and tested at Hiroshima University, Japan under approved animal protocols by Hiroshima University Research Committee. The housing condition is temperature 24-25 degree C, humidity 35-60%, 12 hr dark/light cycle at 8 am and pm.

Note that full information on the approval of the study protocol must also be provided in the manuscript.